Kernels and Integration Cycles in Complex Langevin Simulations

(handout version)

Michael Mandl

with Michael Hansen, Dénes Sexty and Erhard Seiler

based on arXiv:2412.17137

SIGN25 - 23/01/2025

FWF Austrian Science Fund

UNI GRAZ

Handout version*

- This handout is a slightly modified version of the talk given at SIGN 2025. Some additional comments have been added in order to give context to the slides shown.
- Slides marked with an asterisk (*) were not part of the original talk.

The sign problem in lattice QFT

$$\langle \mathcal{O} \rangle = \int dx \mathcal{O}(x) \rho(x)$$

- In Euclidean space, $\rho(x) \propto e^{-S_E(x)}$.
- $\rho(x)$ can be complex:
  - QCD at non-zero density or with a θ term, real-time QFTs, etc.
- Usual lattice approach (importance sampling) not applicable.

The sign problem in lattice QFT*

- We are mainly concerned with the sign problem as it appears in lattice quantum field theory. In particularly, we are interested in Quantum Chromodynamics (QCD) at non-zero (baryon) density, as well as the real-time evolution of quantum field theories. In both cases, the density ρ in the path integral is not real and non-negative, leading to the sign problem. This means that ρ cannot be interpreted as a probabilistic weight and the conventional approach, based on importance sampling, fails.
- As a possible solution, we consider the so-called complex Langevin approach, which is introduced in the following.

Basics of Stochastic Quantization

Parisi, Wu '81; Damgaard, Hüffel '87

- For Euclidean theory in d dimensions, introduce fictitious time direction τ.
- Interpret theory as statistical system coupled to heat reservoir and evolving in τ.
- Obtain target theory $\rho(x) \propto e^{-S(x)}$ in equilibrium limit $\tau \to \infty$.

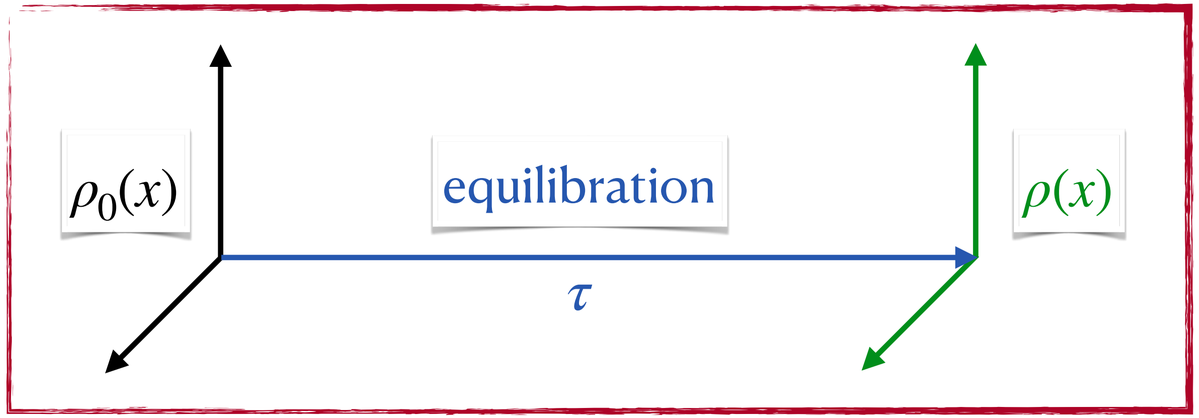

Basics of Stochastic Quantization*

- The idea of stochastic quantization is to interpret the system of interest as a statistical one, which evolves in some fictitious time dimension τ.
- Ideally, one would like to evolve some initial density ρ_0 in τ and obtain the target density $\rho = e^{-S}$ in the equilibrium limit $\tau \to \infty$. For a real action S, this actually works under rather mild assumptions.
- One way to realize this evolution is discussed on the next slide: the τ-evolution of the dynamical degrees of freedom x is given by the Langevin equation, which is a stochastic differential equation consisting of a deterministic part (the drift term) and a stochastic part (the noise). The τ-evolution of the corresponding probability density ρ, in turn, is determined by the associated Fokker-Planck equation. The more interesting question, however, is what happens if the action S is complex.

Langevin and Fokker-Planck equations

Langevin equation

$$\frac{dx}{d\tau} = -\frac{\partial S(x)}{\partial x} + \eta(\tau)$$

drift term

Gaussian noise:

$$\langle \eta(\tau) \rangle = 0$$

$$\langle \eta(\tau)\eta(\tau') \rangle = 2\delta(\tau - \tau')$$

Fokker-Planck equation

$$\frac{\partial \rho(x,\tau)}{\partial \tau} = \frac{\partial}{\partial x}\left(\frac{\partial}{\partial x} + \frac{\partial S(x)}{\partial x}\right)\rho(x,\tau)$$

probability density:

$$\lim_{\tau \to \infty} \rho(x,\tau) \propto e^{-S(x)}$$

Langevin and Fokker-Planck equations

Langevin equation

$$\frac{dx}{d\tau} = -\frac{\partial S(x)}{\partial x} + \eta(\tau)$$

Fokker-Planck equation

$$\frac{\partial \rho(x,\tau)}{\partial \tau} = \frac{\partial}{\partial x}\left(\frac{\partial}{\partial x} + \frac{\partial S(x)}{\partial x}\right)\rho(x,\tau)$$

drift term

Gau

$$\langle \eta(\tau) \rangle = 0$$

$$\langle \eta(\tau)\eta(\tau') \rangle = 2\delta(\tau - \tau')$$

What if $S(x)$ is complex?

density:

$$\lim_{\tau\to\infty} \rho(x,\tau) \propto e^{-S(x)}$$

The complex Langevin equation

Klauder '83; Parisi '83

- Complexify $x \to z = x + \mathrm{i}y$.

Complex Langevin equation

$$\frac{dz}{d\tau} = -\frac{\partial S(z)}{\partial z} + \eta(\tau)$$

- $\Longrightarrow^*$ probability density $P(x, y, \tau)$.
- Does it obey

$$\lim_{\tau\to\infty} \int dxdy\, \mathcal{O}(x + \mathrm{i}y) P(x, y, \tau) = \int dx \mathcal{O}(x)\rho(x)$$

?

The complex Langevin equation*

- The complex Langevin approach — like a few other attempts of solving the sign problem — is based upon the complexification of the underlying field manifold. In this case, we consider a single real variable x and its complex analog z.
- Indeed, the τ-evolution of z produces a probability density $P(x, y, \tau)$ in the complex plane, which — ideally — would reproduce the desired expectation values.
- Notice that, while not discussed in this talk, the complex Langevin equation can be extended to realistic theories like lattice models or gauge theories.

Complex Langevin simulation

- Simulate the process

Discretized evolution equation

$$z_{n+1} = z_n - \varepsilon \left.\frac{\partial S(z)}{\partial z}\right|_{z=z_n} + \sqrt{\varepsilon}\eta_n$$

ε: step size

η_n: real Gaussian noise

- Generate configurations to produce equilibrium distribution for averaging.

Complex Langevin simulation*

- The previous slide shows one (rather simple) way of discretizing the complex Langevin equation, with the discrete (Langevin) time step denoted as ε. Notice the square-root of ε multiplying the Gaussian noise. This update equation can now be used to generate configurations.

Drawbacks and pitfalls

Runaways

$$z \to z - \frac{\partial S(z)}{\partial z}\varepsilon + \sqrt{\varepsilon}\eta$$

- Example: $S(z) = \frac{z^4}{4}$.
- Complexification can introduce runaway trajectories leading to diverging simulation.
- Overcome via adaptive step-size control.

Aarts et al. '10

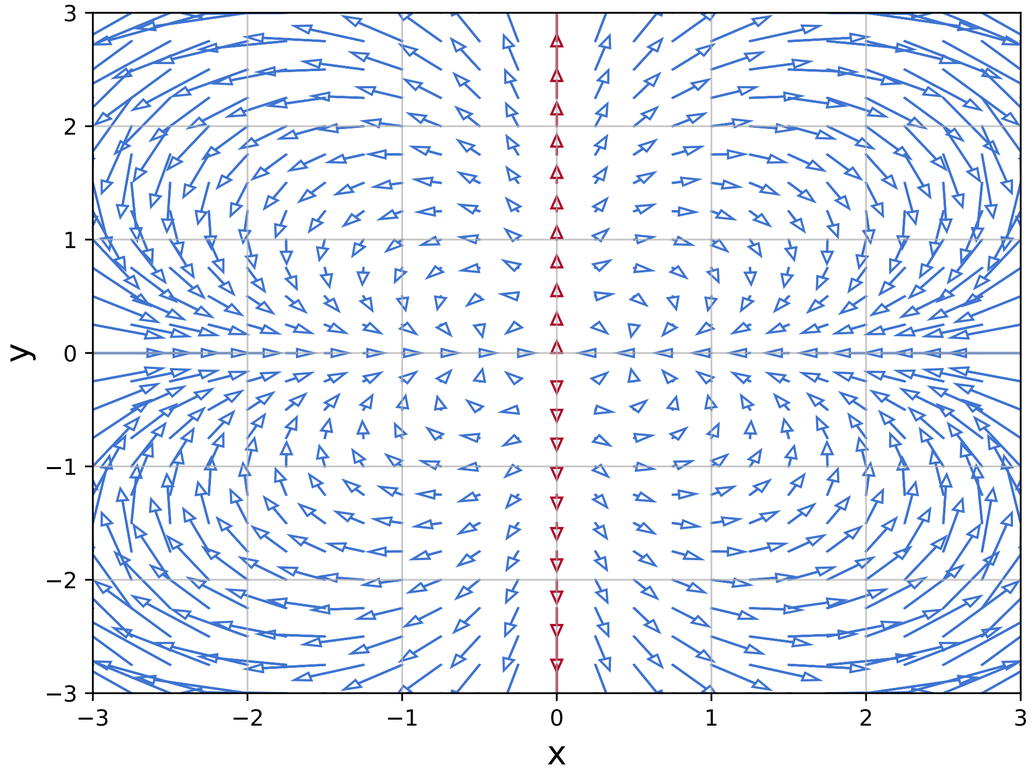

Drawbacks and pitfalls*

Runaways

- One of the drawbacks of the complex Langevin approach is the existence of unstable trajectories, along which the evolution would diverge in the absence of noise.
- In general, the noise term kicks the trajectory off runaway directions, but they might nonetheless bias results if too much time is spent far away from the real axis. In order to reduce discretization effects, one commonly employs an adaptive step-size algorithm to reduce the step size ε when the drift term becomes large, which also partially cures the runaway problem. Either way, the presence of runaways can be detected relatively straightforwardly (for instance by keeping track of the distance to the real axis).

Drawbacks and pitfalls

Wrong convergence

- Complex Langevin simulations can give wrong results despite converging properly.
- Example: $S(z) = \frac{\lambda}{4} z^4, \lambda = e^{\frac{i\pi l}{6}}$.
- Correct convergence only for $|l| \leq 2$.
  Okamoto et al. ’89
- In general, we do not know if results are correct.

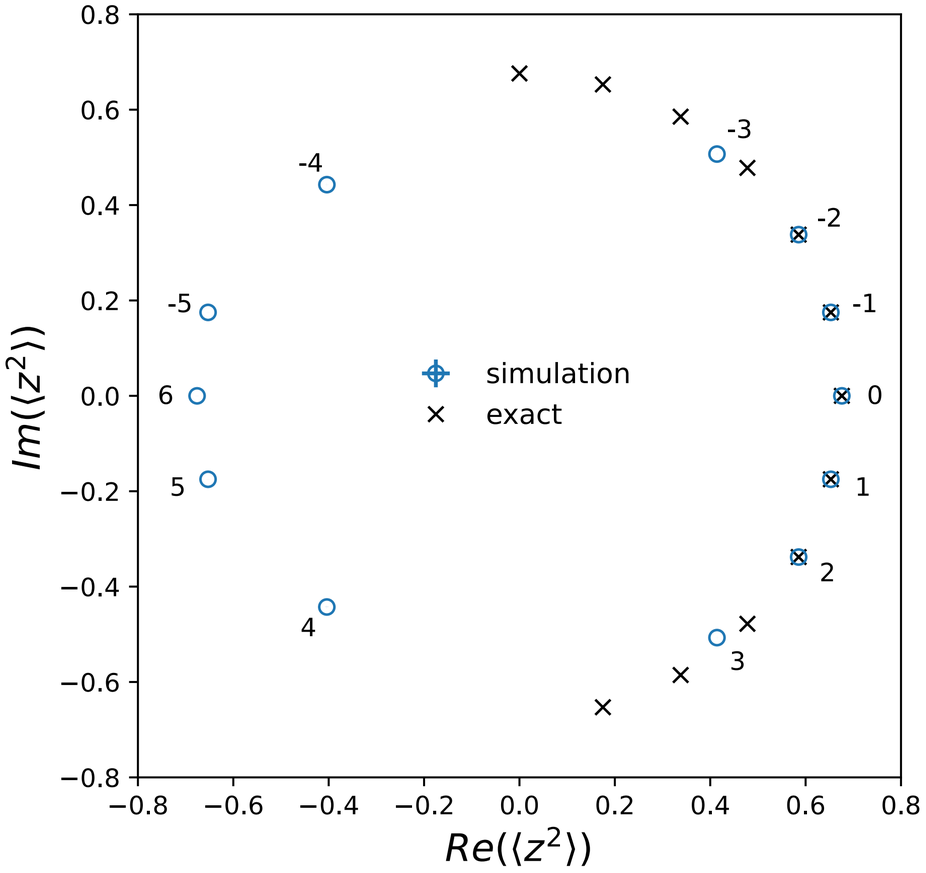

Drawbacks and pitfalls*

Wrong convergence

- On the previous slide, we consider a simple example and compare $\langle z^2 \rangle$, computed both analytically and in a complex Langevin simulation. As this comparison shows, the complex Langevin equation can sometimes produce incorrect solutions despite converging to a proper equilibrium distribution.
- The main problem with this is that — in general — we cannot tell whether the results we obtain in a complex Langevin simulation are correct, since we cannot compare to exact results or to other methods. One thus would like to have some correctness criterion that can distinguish between correct and incorrect results (more on that later).

How to restore correct convergence?

Parisi, Wu ’81; Söderberg ‘88

- May introduce kernel into Langevin equation:

Kernelled complex Langevin equation

$$\frac{dz}{d\tau} = -K(z)\frac{\partial S(z)}{\partial z} + \frac{\partial K(z)}{\partial z} + \sqrt{K(z)}\,\eta(\tau)$$

- For real dynamics: leaves stationary solution of Fokker-Planck equation unchanged.
- Alters the probability distribution $P(x, y, \tau)$.

How to restore correct convergence?*

- In the case of a real action, one can introduce a so-called kernel $K(z)$ into the Langevin equation, which (again, under mild assumptions) leaves the resulting equilibrium distribution e^{-S} intact, but might improve convergence properties.
- For complex actions, however, the kernel can affect the distribution P in the complex plane, which might be desirable if correct convergence cannot be achieved without a kernel.
- While the kernel can be z-dependent in general, we choose it to be constant here for simplicity.
- On the next few slides we demonstrate the effect of a simple kernel on the distribution of z in the complex plane, using a very simple example.

Complex Langevin evolution with a kernel

$$z \to z - \varepsilon K \frac{\partial S(z)}{\partial z} + \sqrt{\varepsilon K}\,\eta$$

- Example: $S(z) = \frac{\lambda}{4} z^4$, $\lambda = e^{\frac{5i\pi}{6}}$, $K = e^{-\frac{i\pi m}{24}}$.

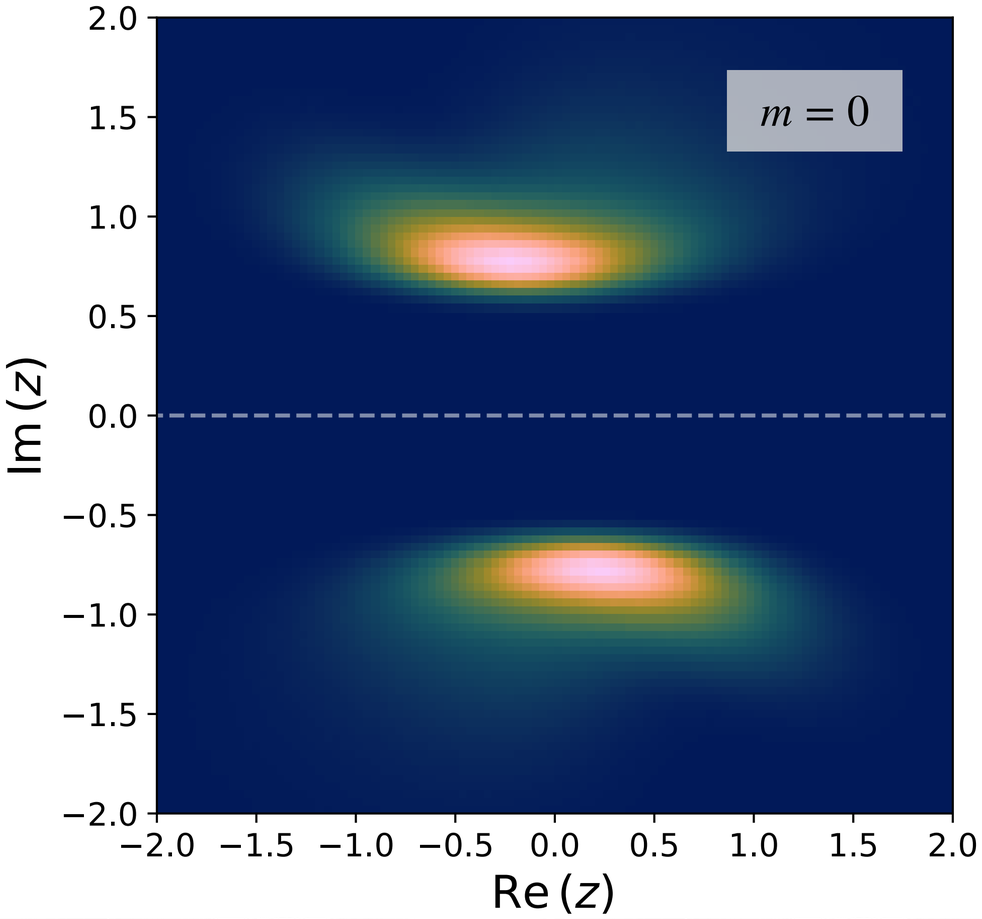

Complex Langevin evolution with a kernel

$$z \to z - \varepsilon K \frac{\partial S(z)}{\partial z} + \sqrt{\varepsilon K}\,\eta$$

- Example: $S(z) = \frac{\lambda}{4} z^4$, $\lambda = e^{\frac{5i\pi}{6}}$, $K = e^{-\frac{i\pi m}{24}}$.

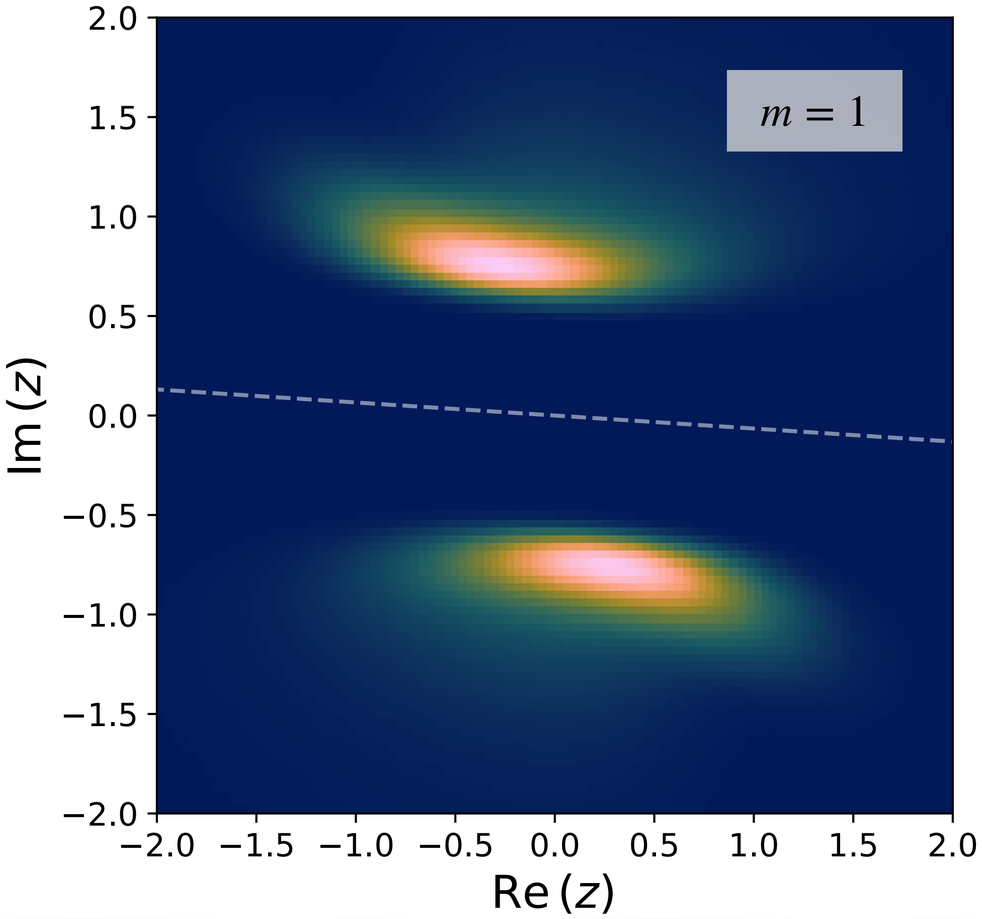

Complex Langevin evolution with a kernel

$$z \to z - \varepsilon K \frac{\partial S(z)}{\partial z} + \sqrt{\varepsilon K}\,\eta$$

- Example: $S(z) = \frac{\lambda}{4} z^4$, $\lambda = e^{\frac{5i\pi}{6}}$, $K = e^{-\frac{i\pi m}{24}}$.

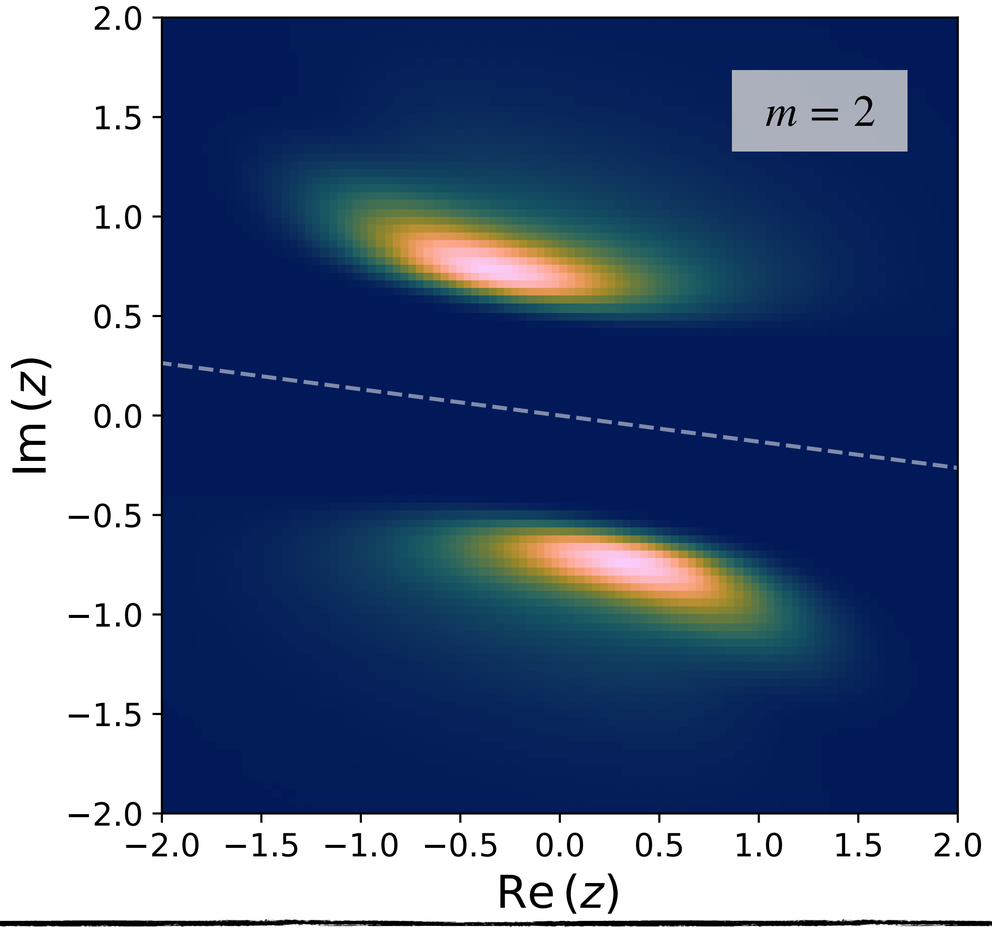

Complex Langevin evolution with a kernel

$$z \to z - \varepsilon K \frac{\partial S(z)}{\partial z} + \sqrt{\varepsilon K}\,\eta$$

- Example: $S(z) = \frac{\lambda}{4} z^4$, $\lambda = e^{\frac{5i\pi}{6}}$, $K = e^{-\frac{i\pi m}{24}}$.

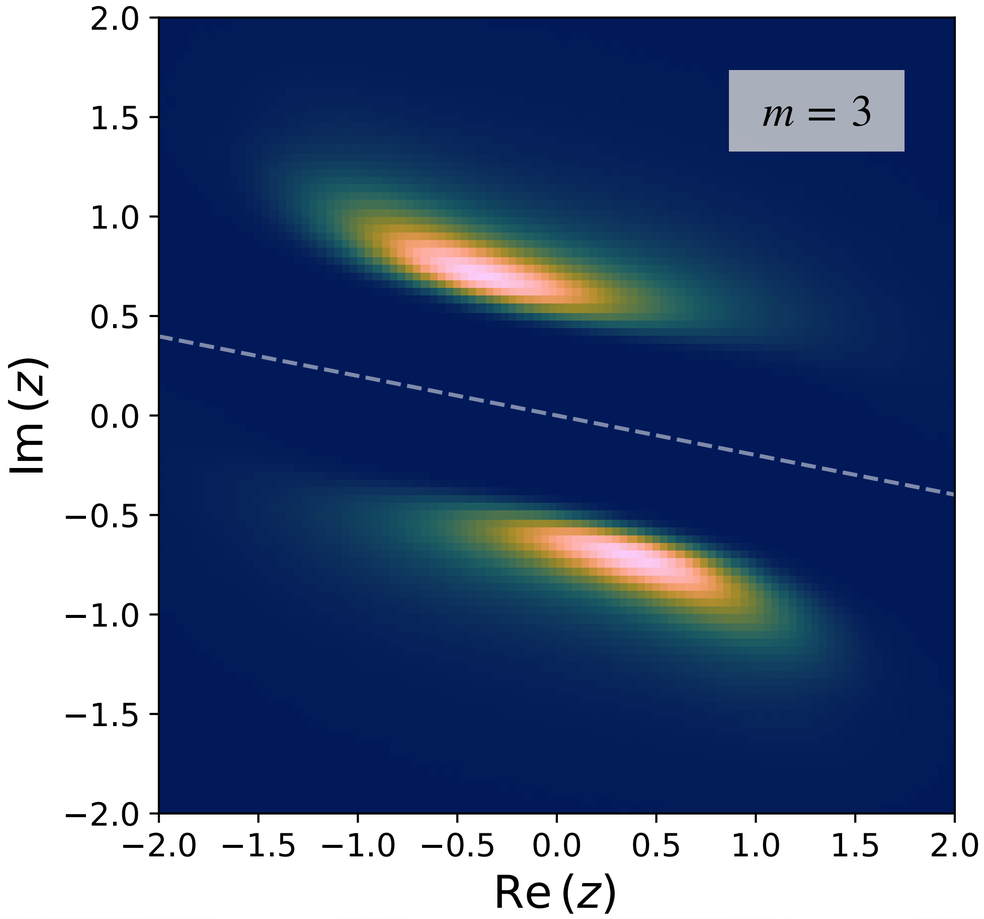

Complex Langevin evolution with a kernel

$$z \to z - \varepsilon K \frac{\partial S(z)}{\partial z} + \sqrt{\varepsilon K}\,\eta$$

- Example: $S(z) = \frac{\lambda}{4} z^4$, $\lambda = e^{\frac{5i\pi}{6}}$, $K = e^{-\frac{i\pi m}{24}}$.

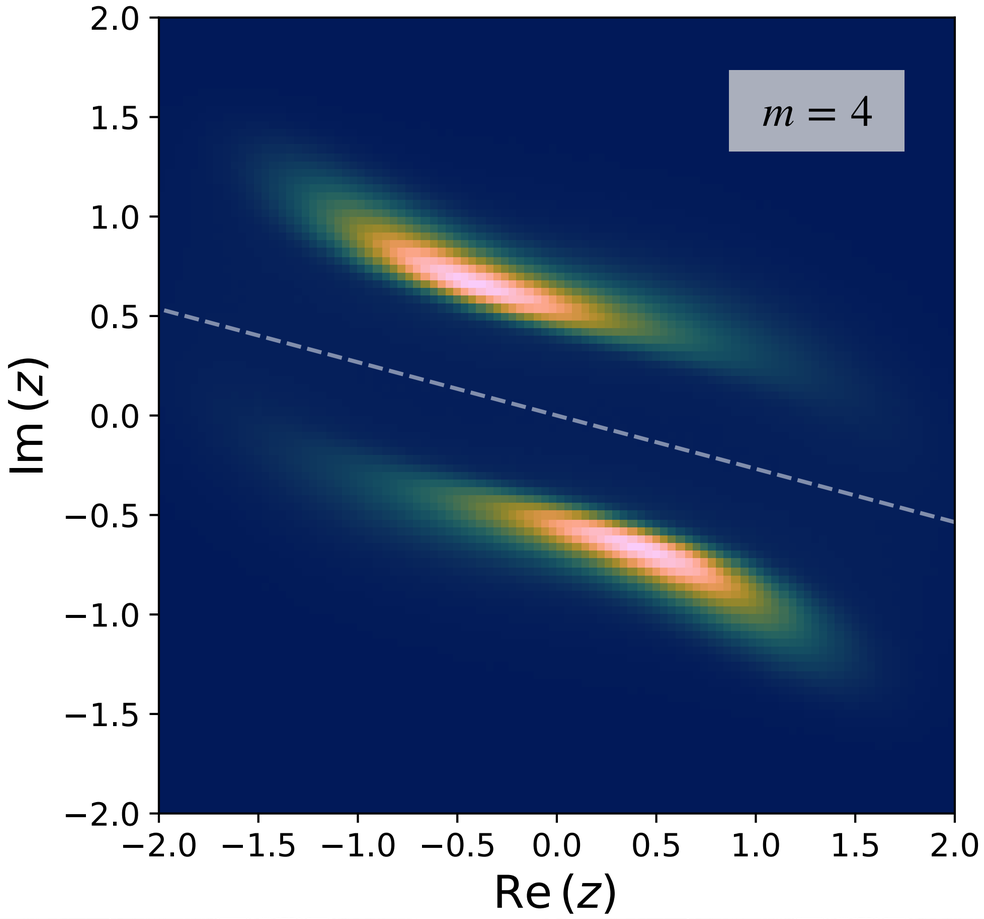

Complex Langevin evolution with a kernel

$$z \to z - \varepsilon K \frac{\partial S(z)}{\partial z} + \sqrt{\varepsilon K}\,\eta$$

- Example: $S(z) = \frac{\lambda}{4} z^4$, $\lambda = e^{\frac{5i\pi}{6}}$, $K = e^{-\frac{i\pi m}{24}}$.

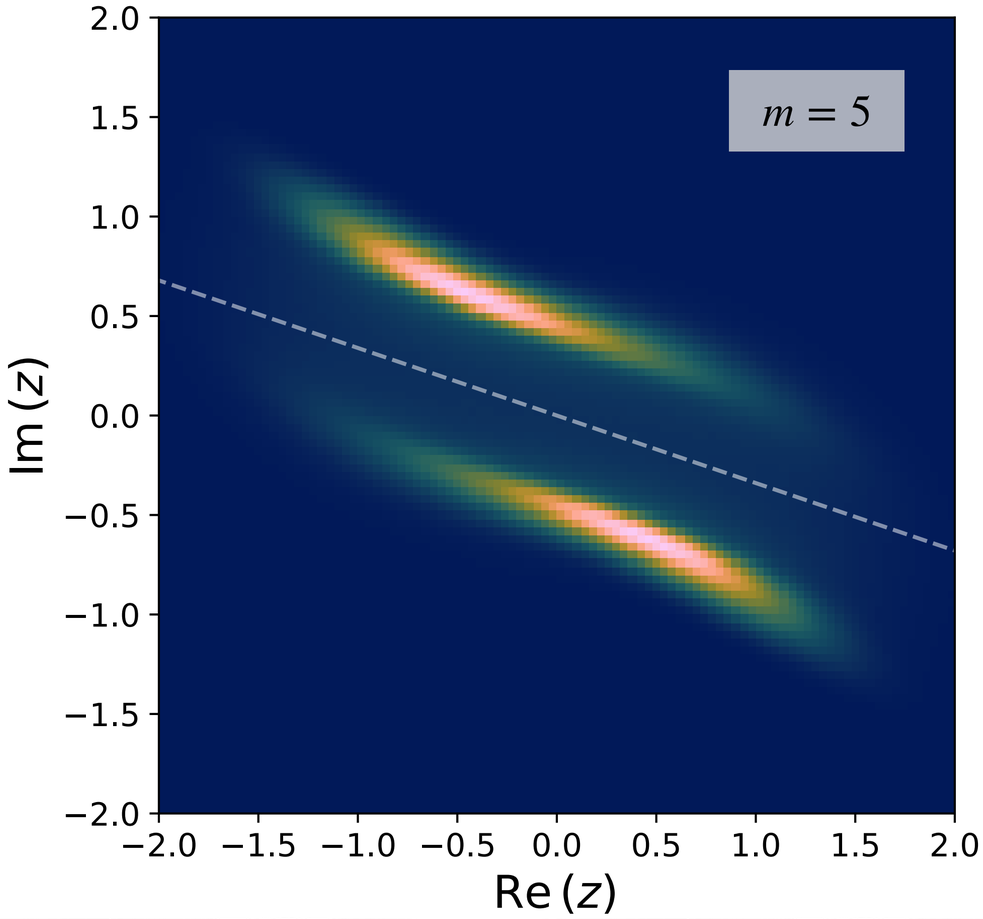

Complex Langevin evolution with a kernel

$$z \to z - \varepsilon K \frac{\partial S(z)}{\partial z} + \sqrt{\varepsilon K}\,\eta$$

- Example: $S(z) = \frac{\lambda}{4} z^4$, $\lambda = e^{\frac{5i\pi}{6}}$, $K = e^{-\frac{i\pi m}{24}}$.

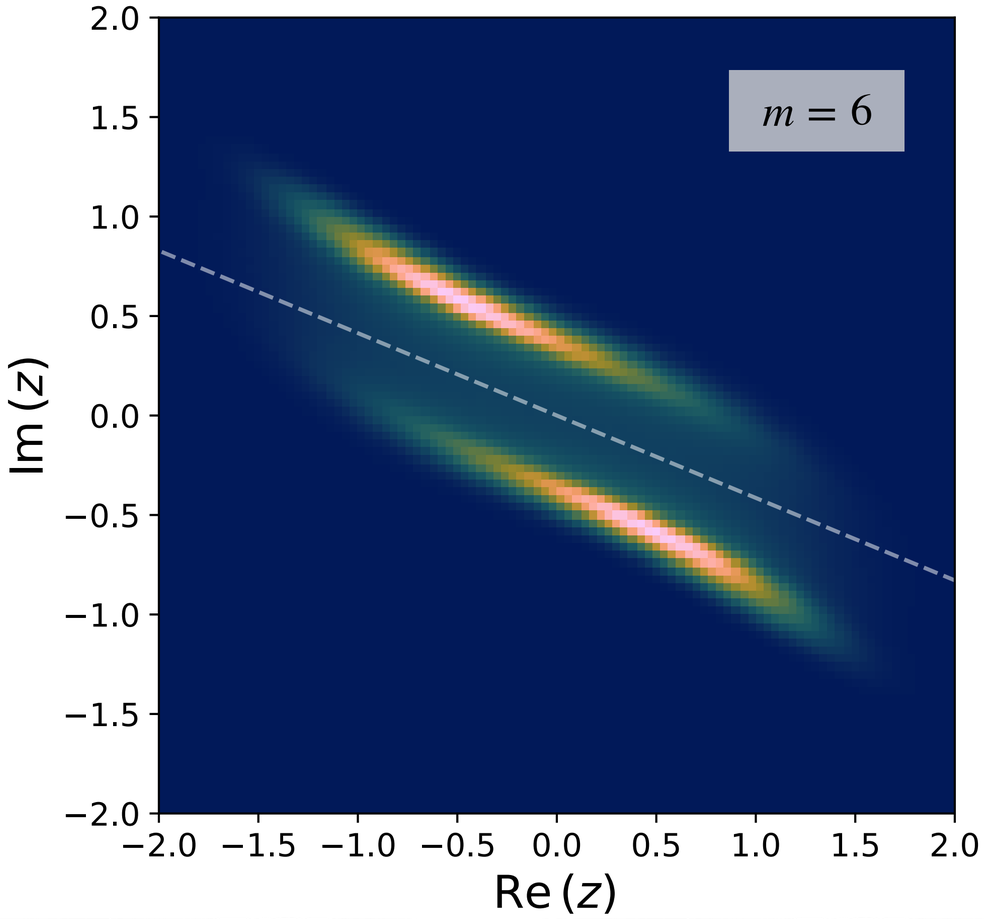

Complex Langevin evolution with a kernel

$$z \to z - \varepsilon K \frac{\partial S(z)}{\partial z} + \sqrt{\varepsilon K}\,\eta$$

- Example: $S(z) = \frac{\lambda}{4} z^4$, $\lambda = e^{\frac{5i\pi}{6}}$, $K = e^{-\frac{i\pi m}{24}}$.

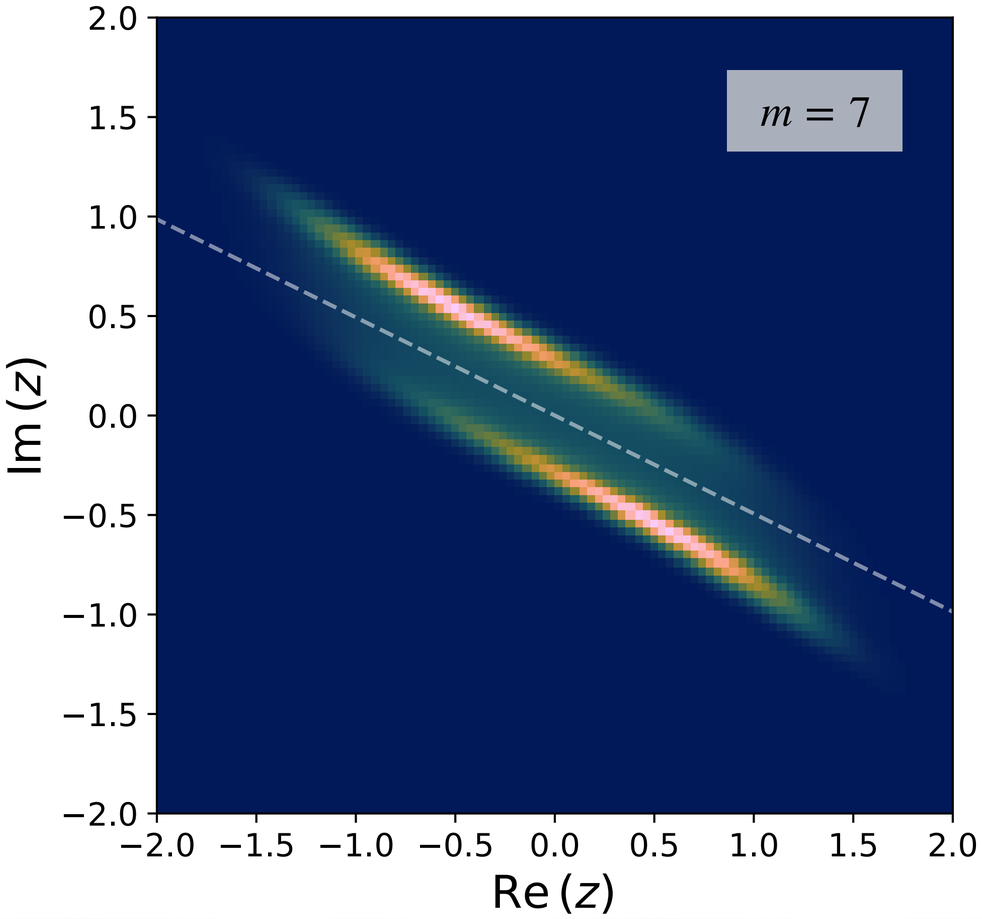

Complex Langevin evolution with a kernel

$$z \to z - \varepsilon K \frac{\partial S(z)}{\partial z} + \sqrt{\varepsilon K}\,\eta$$

- Example: $S(z) = \frac{\lambda}{4} z^4$, $\lambda = e^{\frac{5i\pi}{6}}$, $K = e^{-\frac{i\pi m}{24}}$.

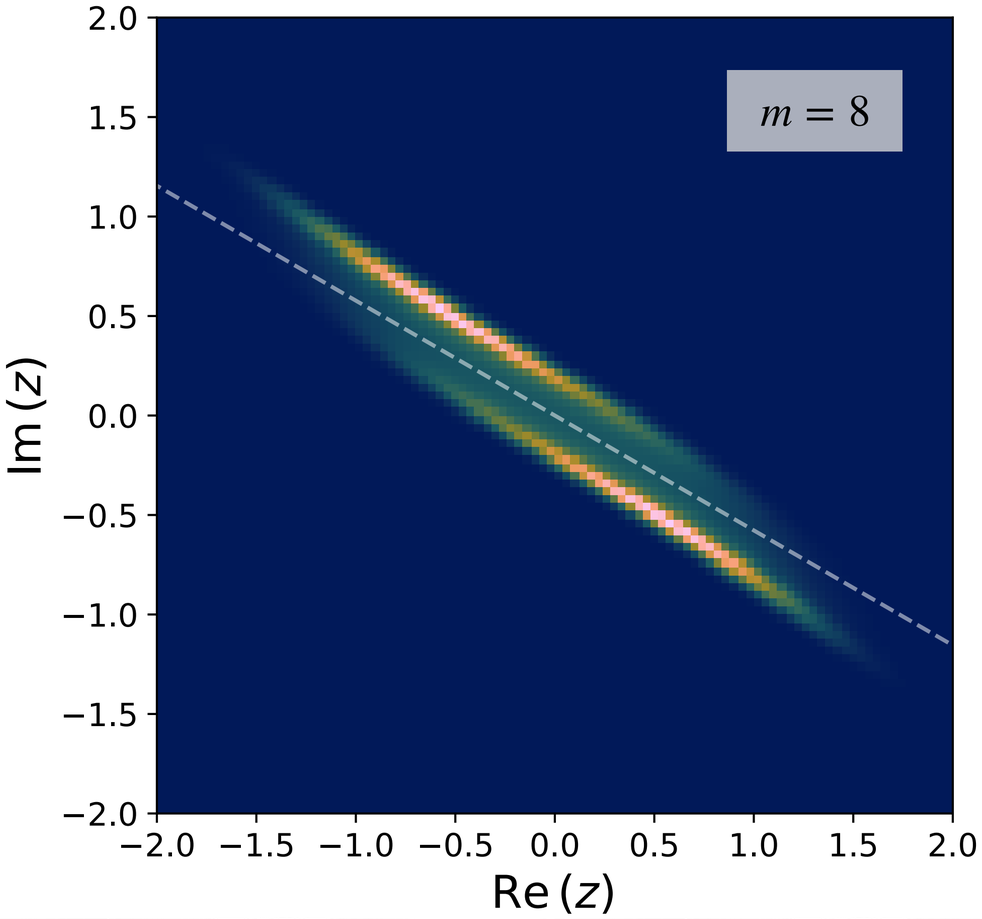

Complex Langevin evolution with a kernel

$$z \to z - \varepsilon K \frac{\partial S(z)}{\partial z} + \sqrt{\varepsilon K}\,\eta$$

- Example: $S(z) = \frac{\lambda}{4} z^4$, $\lambda = e^{\frac{5i\pi}{6}}$, $K = e^{-\frac{i\pi m}{24}}$.

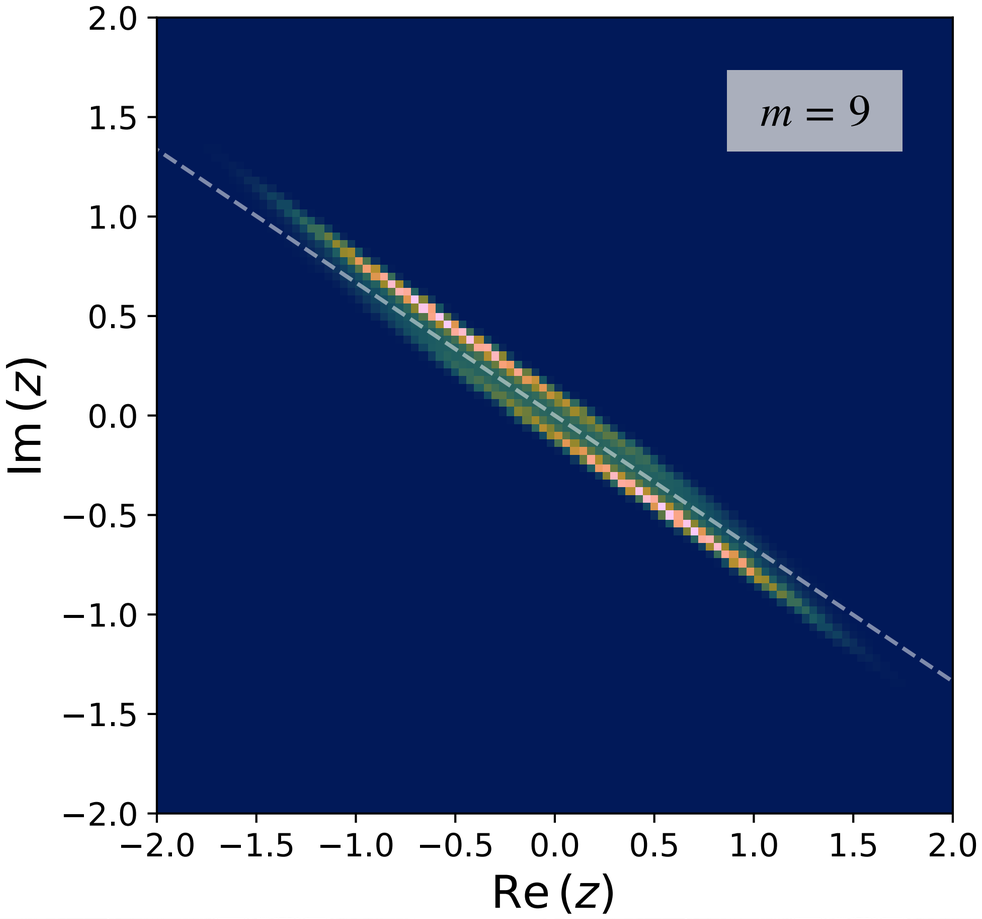

Complex Langevin evolution with a kernel

$$z \to z - \varepsilon K \frac{\partial S(z)}{\partial z} + \sqrt{\varepsilon K}\,\eta$$

- Example: $S(z) = \frac{\lambda}{4} z^4$, $\lambda = e^{\frac{5i\pi}{6}}$, $K = e^{-\frac{i\pi m}{24}}$.

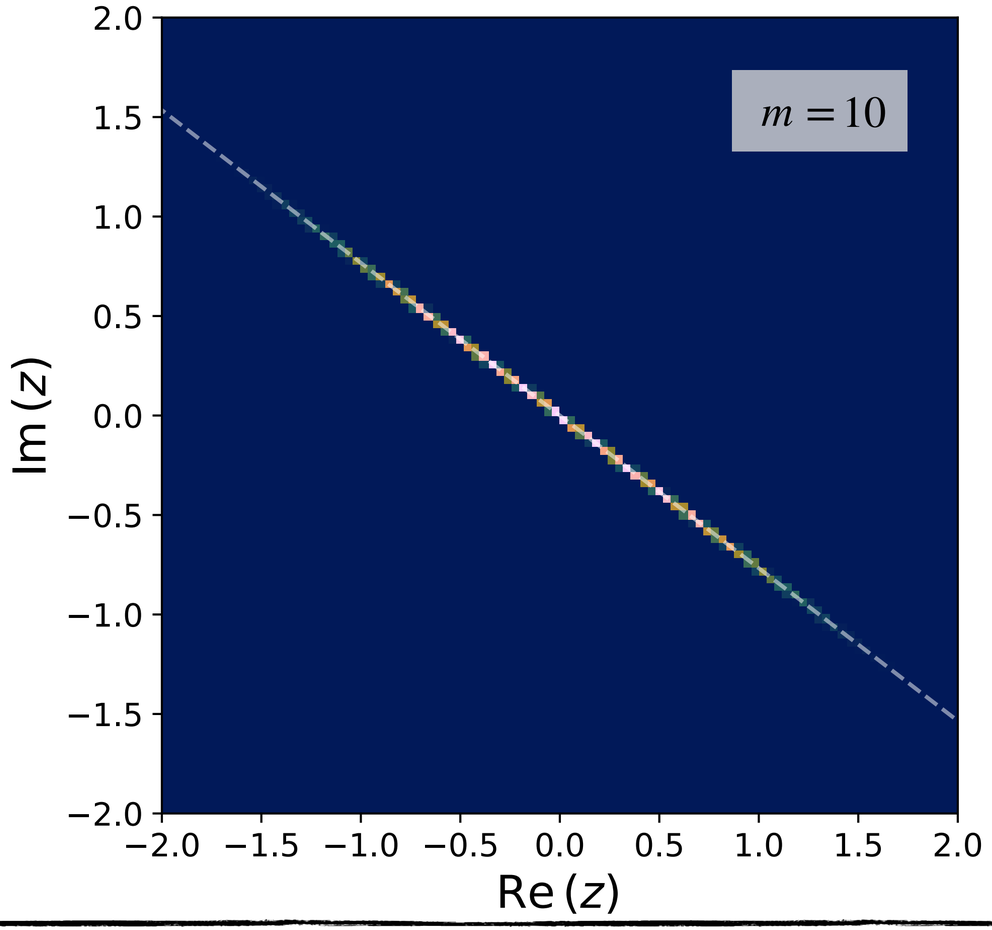

Complex Langevin evolution with a kernel*

- Indeed, the kernel affects the distribution in several ways. Most strikingly, the distribution follows the direction noise coefficient $\sqrt{K}$ (dashed lines). This leads to the interesting observation that for $m = 10$ the distribution collapses to a line, namely the relevant Lefschetz thimble of the theory. One may guess that in that case one may obtain correct results, which is demonstrated on the next slide, where the observable $\langle z^2 \rangle$ is shown as a function of the kernel parameter m.
- Indeed, there are large plateaus in m, one of which lies around $m = 10$. On this plateau, complex Langevin results agree with the exact ones. On the other plateaus, however, results are incorrect.

Complex Langevin evolution with a kernel

$$z \to z - \varepsilon K \frac{\partial S(z)}{\partial z} + \sqrt{\varepsilon K}\,\eta$$

- Example: $S(z) = \frac{\lambda}{4} z^4$, $\lambda = e^{\frac{5i\pi}{6}}$, $K = e^{-\frac{i\pi m}{24}}$.
- Kernel can restore correct convergence.
  Okamoto et al. '89
- Want: Correctness criterion.

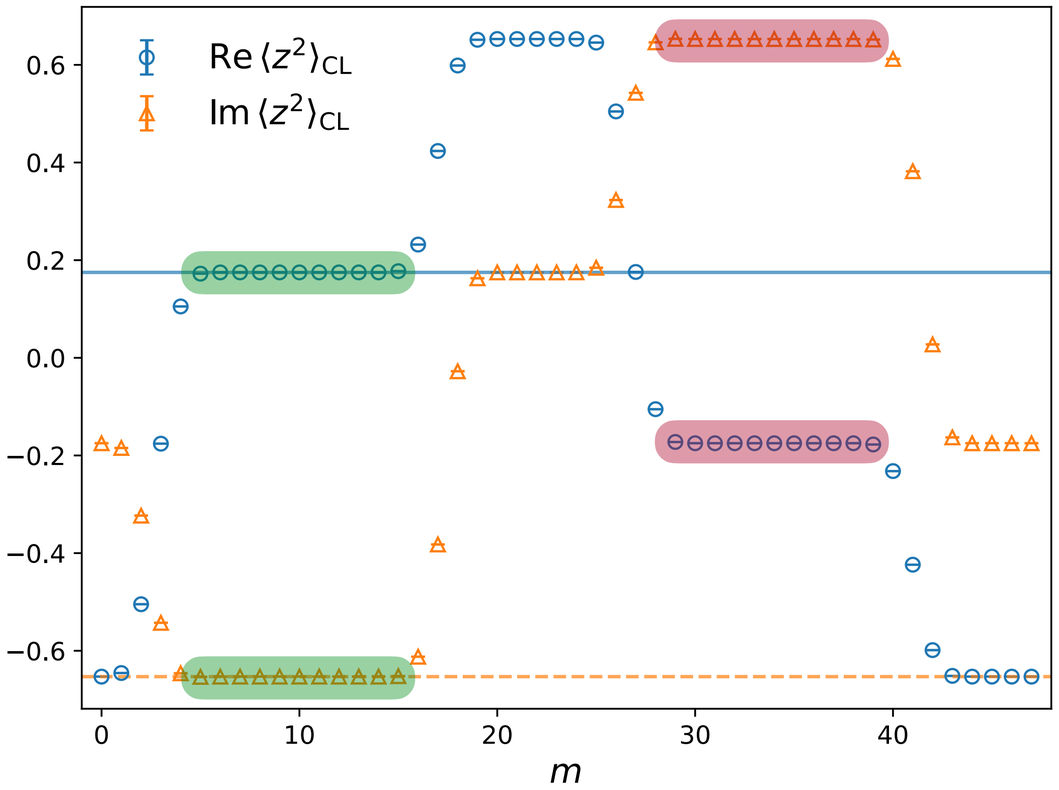

Boundary terms

Aarts et al. ’11; Scherzer et al. ‘19

- Formal argument for correctness relies on fast decay of $P\mathcal{O}$, such that one can integrate by parts without appearance of boundary terms.
- Can measure boundary terms

$$B_{\mathcal{O}(z)}(Y) = \left\langle \Theta\left(Y - |z|\right) L\mathcal{O}(z) \right\rangle$$

Boundary terms*

Boundary terms*

- The formal proof of correctness of the complex Langevin approach relies on the absence of boundary terms such that one can integrate by parts. In practice, one may measure boundary terms via the observable given on the previous slide.
- In particular, one plots the boundary terms B as a function of the cutoff Y and looks for a plateau. If such a plateau appears at a non-vanishing value or if no signs of a plateau can be found at all, this implies that the simulation results are incorrect. Examples for boundary terms for different values of m are shown on the next slide. There, we also see that the converse statement is not true: the absence of boundary terms does not ensure the correctness of results. An explanation for this is provided in the slides that follow.

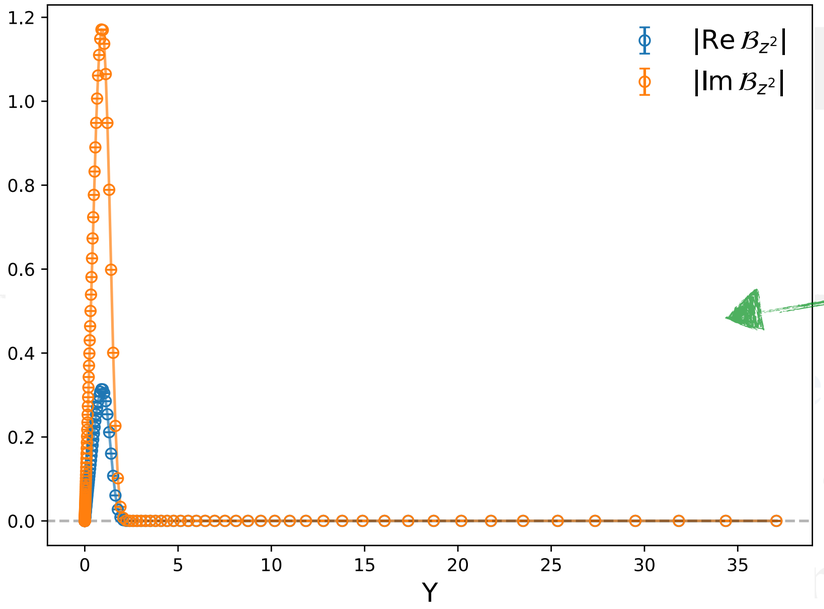
|Re $\mathcal{B}_{z^2}$|
|Im $\mathcal{B}_{z^2}$|
Y

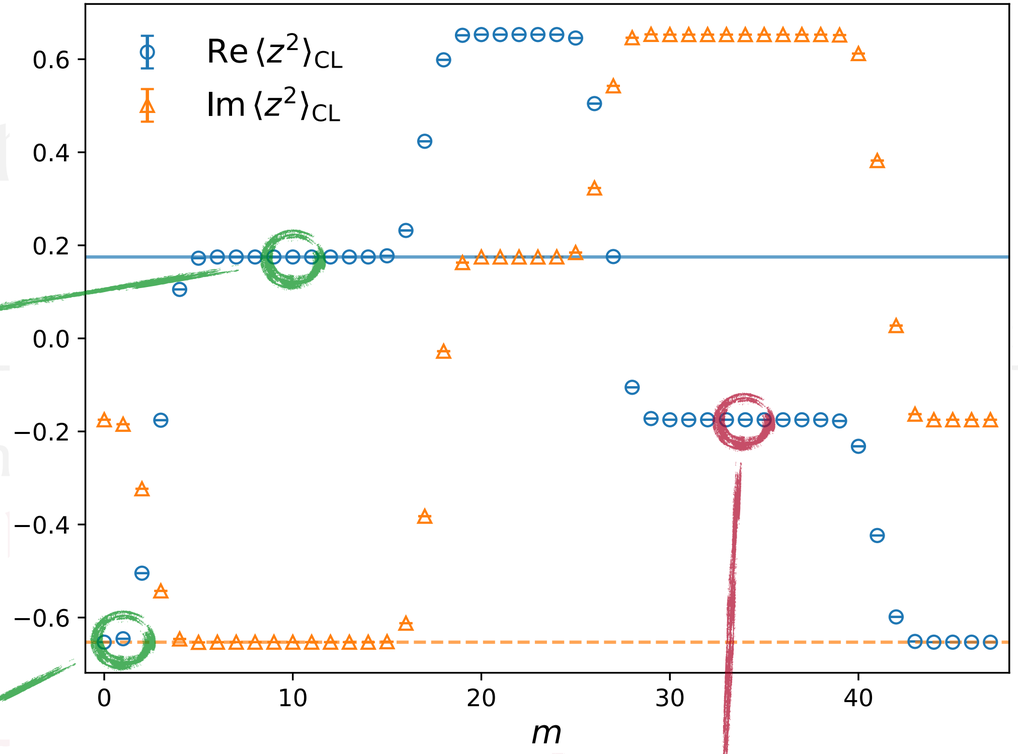
Re $\langle z^2 \rangle_{CL}$
Im $\langle z^2 \rangle_{CL}$
m

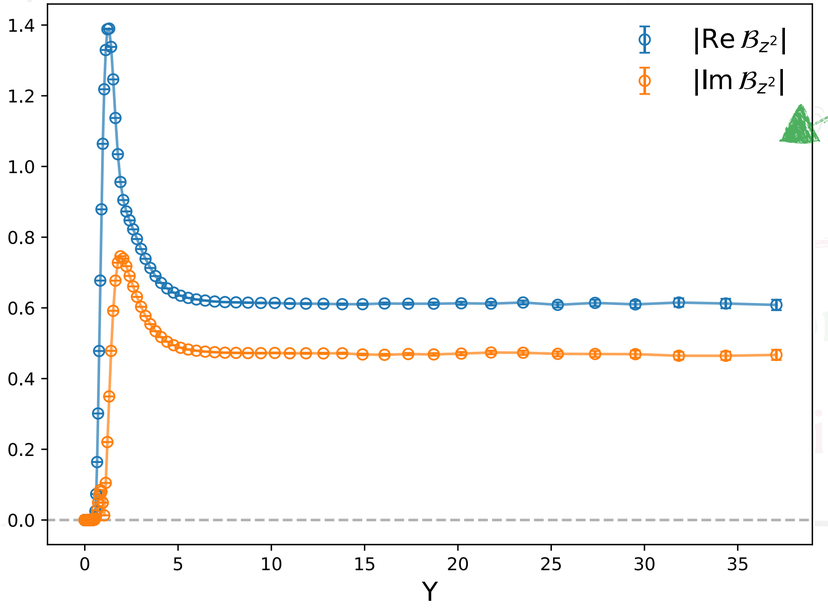
|Re $\mathcal{B}_{z^2}$|
|Im $\mathcal{B}_{z^2}$|
Y

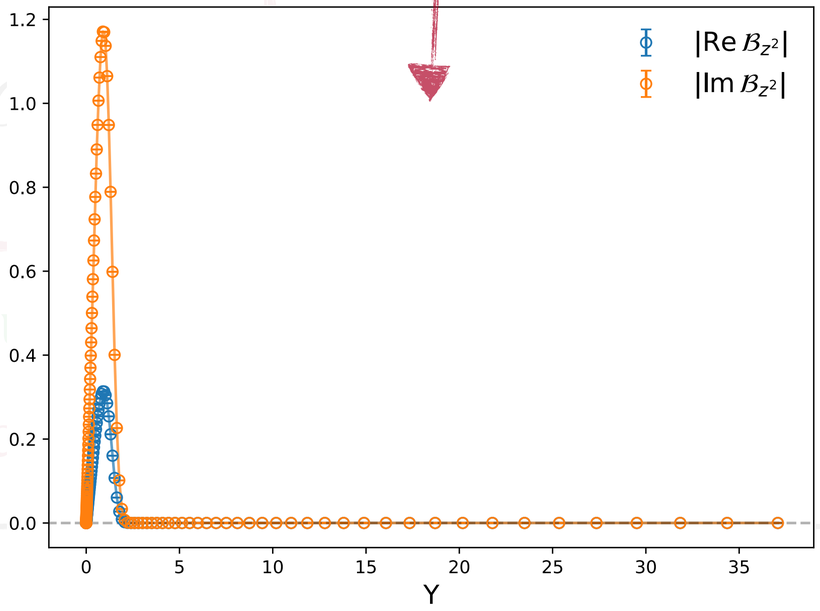
|Re $\mathcal{B}_{z^2}$|
|Im $\mathcal{B}_{z^2}$|
Y

Boundary terms

Aarts et al. ’11; Scherzer et al. ‘19

- Formal argument for correctness relies on fast decay of $P\mathcal{O}$, such that one can integrate by parts without appearance of boundary terms.
- Can measure boundary terms

$$B_{\mathcal{O}(z)}(Y) = \left\langle \Theta\left(Y - |z|\right) L\mathcal{O}(z) \right\rangle$$

- Can infer incorrect solutions from non-vanishing boundary terms.
- Cannot infer correct solutions from vanishing boundary terms.

Integration cycles

Witten ‘11

- Integration paths connecting zeros of $\rho(z)$.
- Example: $\rho(z) = e^{-\frac{z^4}{4}}$.
- Three independent cycles, γ_1 is the relevant one.
- Vanishing boundary terms only imply that result is linear combination of integration cycles:

$$\langle \mathcal{O} \rangle_{\text{CL}} = \sum_{i=1}^{3} a_i \langle \mathcal{O} \rangle_{\gamma_i}$$

Salcedo, Seiler ’19

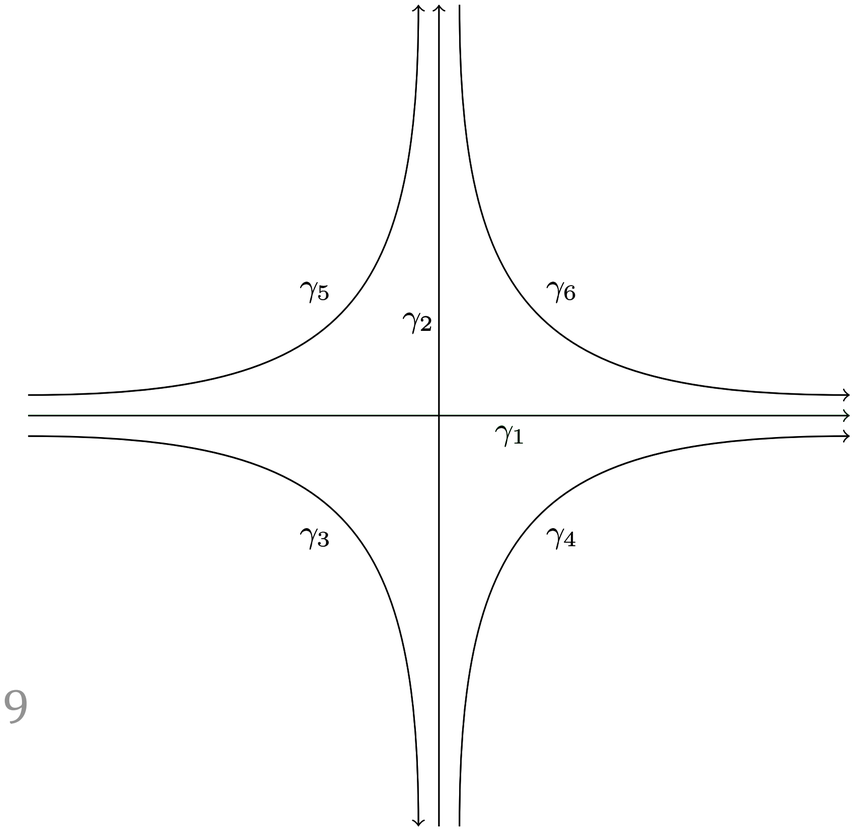

Integration cycles*

- The absence of boundary terms does not guarantee the correctness of results, which is especially true in the presence of a kernel. An explanation for this (in one-dimensional theories) was put forward by Salcedo and Seiler, in that the absence of boundary terms only implies that the complex-Langevin results are a linear combination of observables computed along different integration cycles, $\langle \mathcal{O} \rangle_{\gamma_i}$.
- An integration cycle is an integration path in the complex plane that either connects two distinct zeros of e^{-S} or is a closed non-contractible loop (the latter do not play a role in this talk). The integral over the real line, which is the one we are interested in, is only one such integration cycle, but in general we should expect other cycles to contribute as well. For the particular model considered, there are (up to inversion) six possible integration cycles, only three of which, however, are linearly independent.

Kernel and integration cycles

$$\langle \mathcal{O} \rangle_{\mathrm{CL}} = \sum_{i=1}^{3} a_i \langle \mathcal{O} \rangle_{\gamma_i}$$

- Kernel can favor certain cycles.
  Salcedo '93
- Fits are unreliable in the presence of boundary terms.
- Only proven for a single degree of freedom.

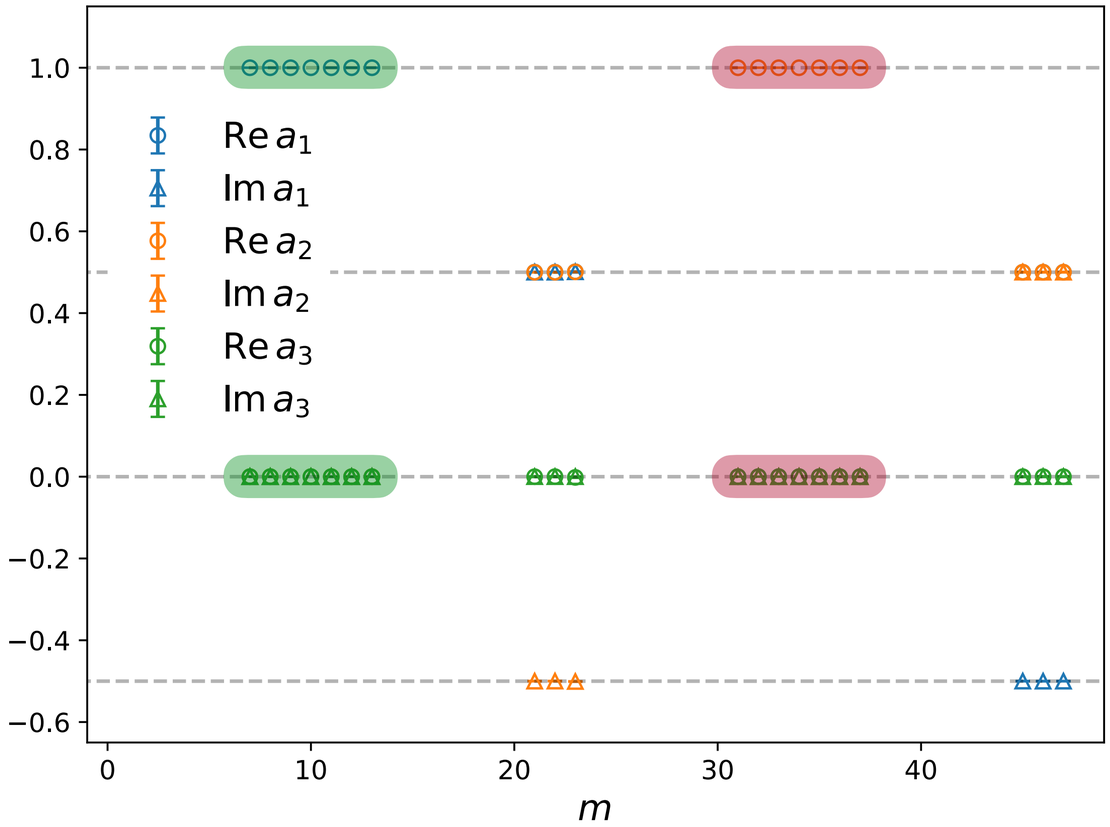

Kernel and integration cycles*

- Owing to the simplicity of the models considered here, we may actually compute the coefficients a_i via a least-squares fit, since we can compute the $\langle \mathcal{O} \rangle_{\gamma_i}$ exactly. The result of this fit as a function of m is shown on the previous slide. Indeed, we find $a_i = \delta_{i1}$ close to $m = 10$, while on the other plateaus different linear combinations of cycles become relevant. Away from the plateaus the fits become unstable, namely precisely for those kernels where there are boundary terms, which perfectly confirms the theorem by Salcedo and Seiler. Notice that a_3 always vanishes for this choice of kernel.
- So far, however, the theorem has been proven only in one dimension. Here, we thus study its validity in two dimensions from a numerical point of view.

Higher dimensions*

- The generalization of the complex Langevin equation to higher dimensions is straightforward. On the next few slides, we repeat the steps discussed before in a simple two-dimensional model. Notice that, while the kernel can be a matrix in general, we choose it to be proportional to unity here. We show the distributions of the z_i (which coincide) in the complex plane for different kernel parameters m, as well as the m-dependence of the observable $\langle z_1^2 \rangle$ (other observables look similar).
- The conclusions are also similar to the one-dimensional case, the main difference being that the two smaller plateaus are absent in two dimensions.

Higher dimensions

$$z_i \to z_i - \varepsilon K \frac{\partial S(z_1, z_2)}{\partial z_i} + \sqrt{\varepsilon K}\,\eta_i$$

- Consider $S(z_1, z_2) = \frac{\lambda}{4}(z_1^2 + z_2^2)^2$.
- Example: $\lambda = e^{\frac{5i\pi}{6}}$, $K = e^{-\frac{i\pi m}{24}}$.

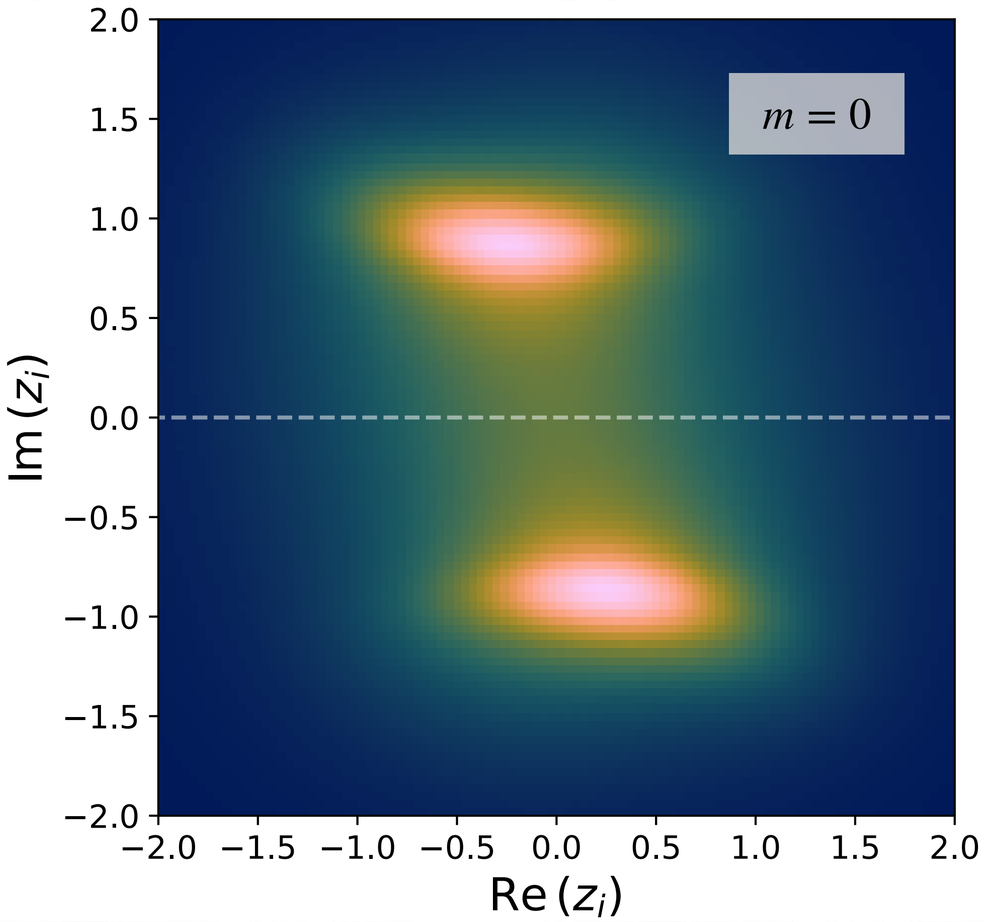

Higher dimensions

$$z_i \to z_i - \varepsilon K \frac{\partial S(z_1, z_2)}{\partial z_i} + \sqrt{\varepsilon K}\,\eta_i$$

- Consider $S(z_1, z_2) = \frac{\lambda}{4}(z_1^2 + z_2^2)^2$.
- Example: $\lambda = e^{\frac{5i\pi}{6}}$, $K = e^{-\frac{i\pi m}{24}}$.

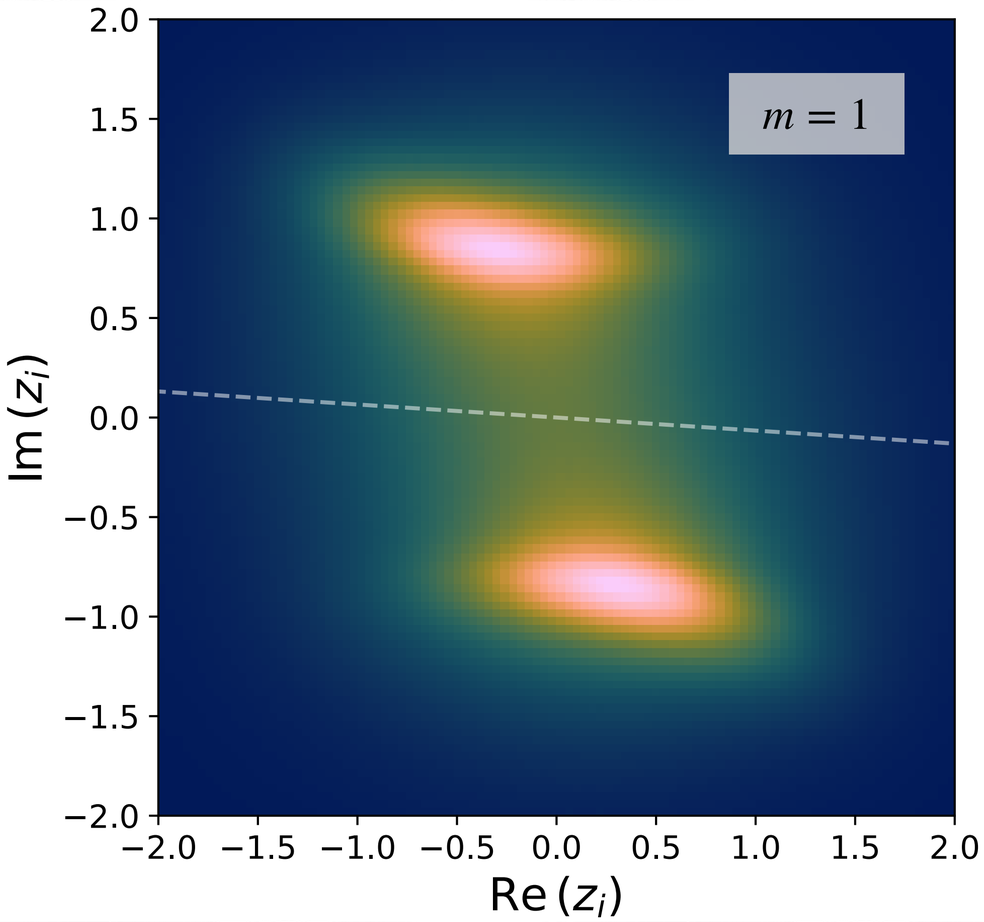

Higher dimensions

$$z_i \to z_i - \varepsilon K \frac{\partial S(z_1, z_2)}{\partial z_i} + \sqrt{\varepsilon K}\,\eta_i$$

- Consider $S(z_1, z_2) = \frac{\lambda}{4}(z_1^2 + z_2^2)^2$.
- Example: $\lambda = e^{\frac{5i\pi}{6}}$, $K = e^{-\frac{i\pi m}{24}}$.

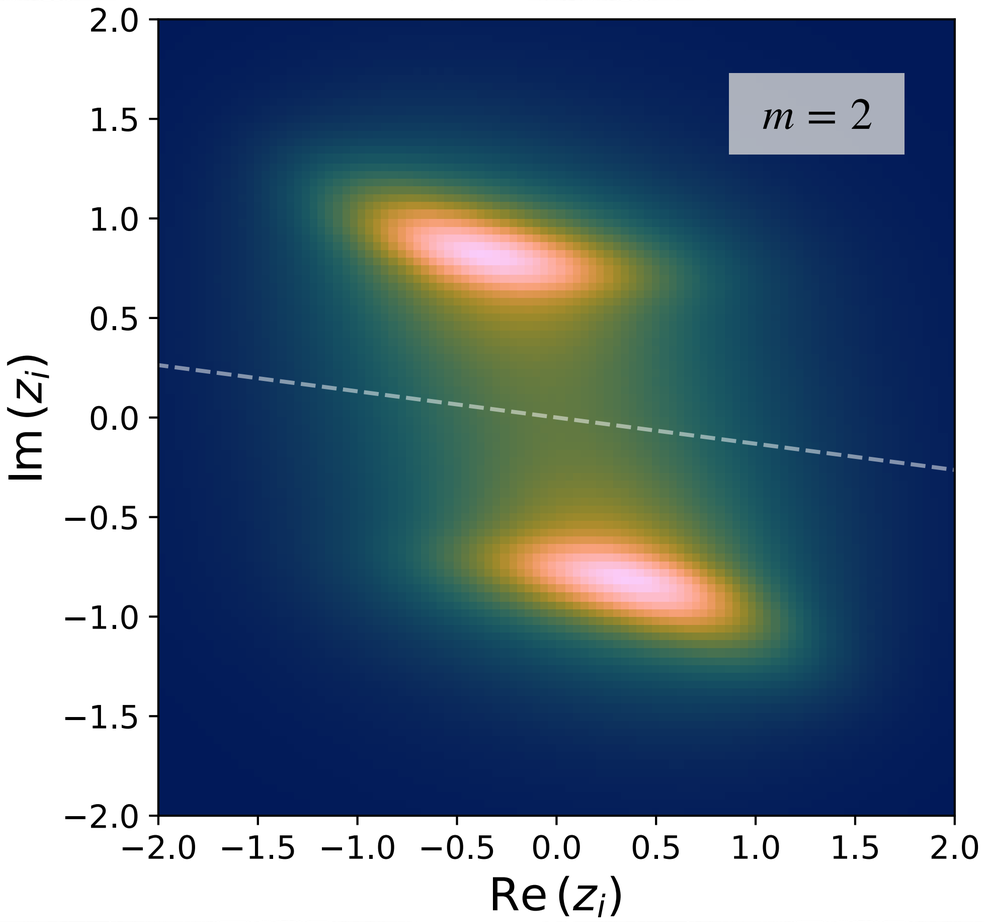

Higher dimensions

$$z_i \to z_i - \varepsilon K \frac{\partial S(z_1, z_2)}{\partial z_i} + \sqrt{\varepsilon K}\,\eta_i$$

- Consider $S(z_1, z_2) = \frac{\lambda}{4}(z_1^2 + z_2^2)^2$.
- Example: $\lambda = e^{\frac{5i\pi}{6}}$, $K = e^{-\frac{i\pi m}{24}}$.

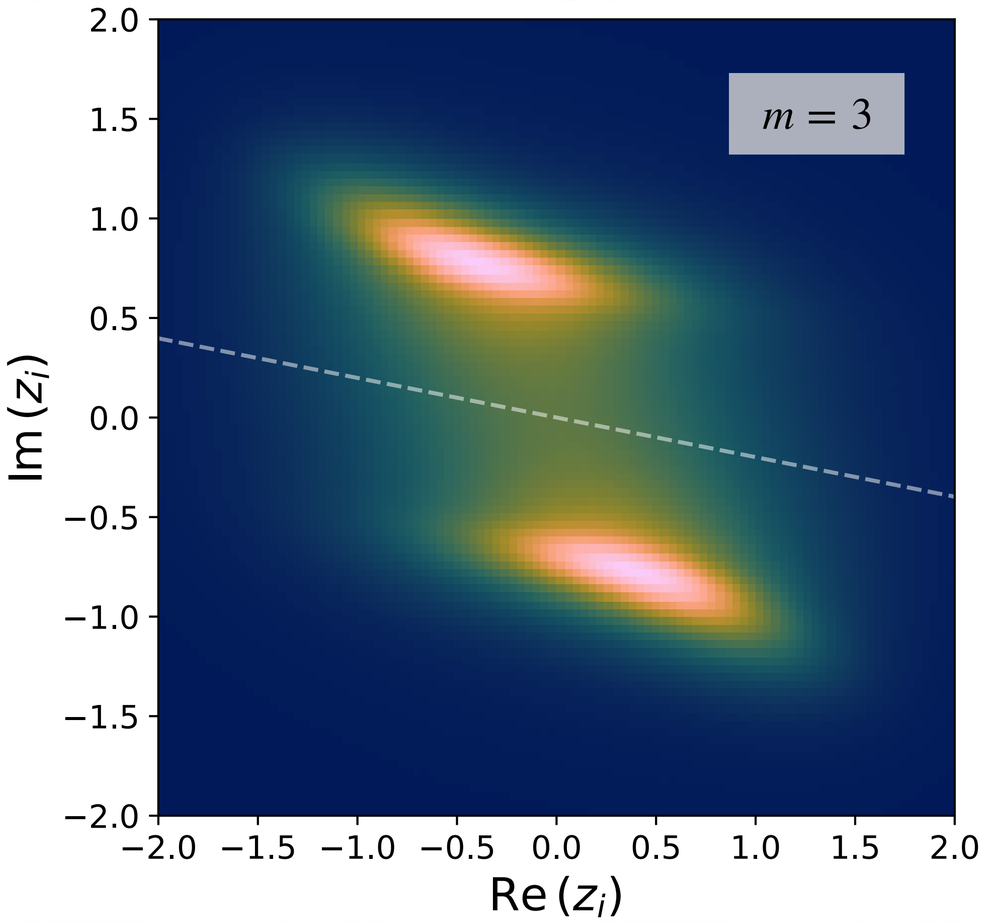

Higher dimensions

$$z_i \to z_i - \varepsilon K \frac{\partial S(z_1, z_2)}{\partial z_i} + \sqrt{\varepsilon K}\,\eta_i$$

- Consider $S(z_1, z_2) = \frac{\lambda}{4}(z_1^2 + z_2^2)^2$.
- Example: $\lambda = e^{\frac{5i\pi}{6}}$, $K = e^{-\frac{i\pi m}{24}}$.

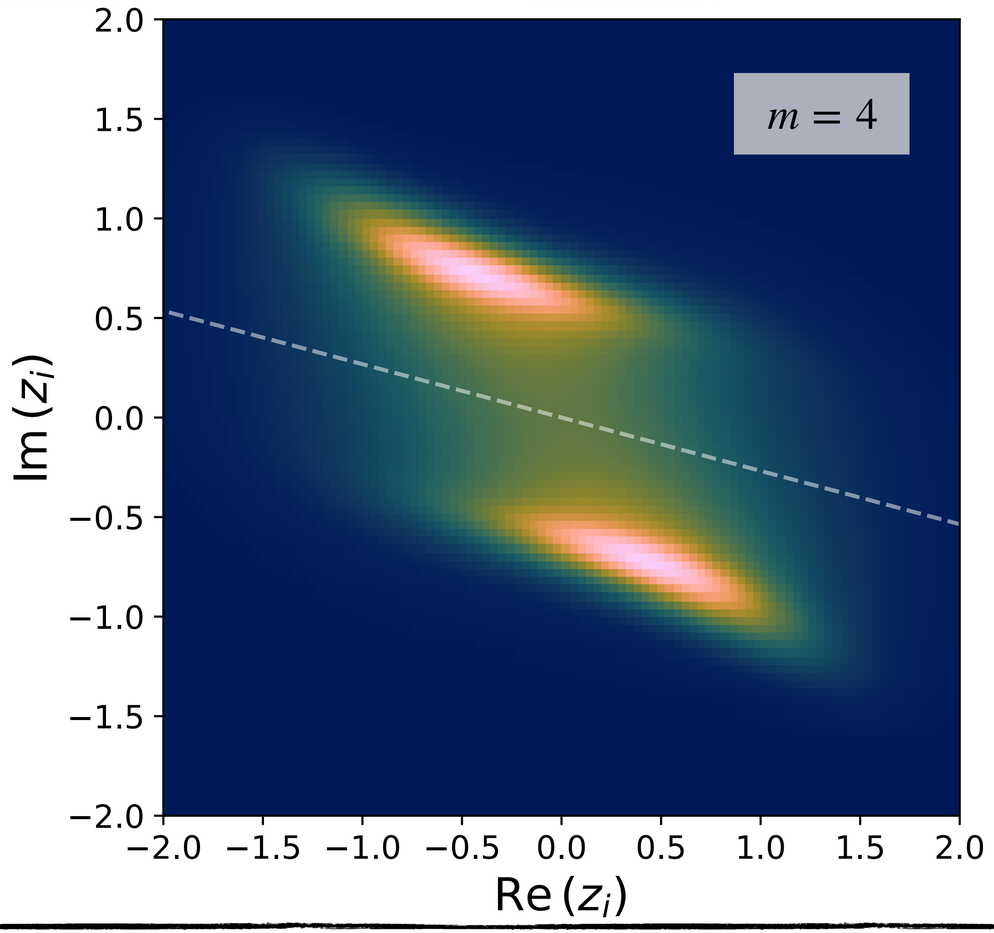

Higher dimensions

$$z_i \to z_i - \varepsilon K \frac{\partial S(z_1, z_2)}{\partial z_i} + \sqrt{\varepsilon K}\,\eta_i$$

- Consider $S(z_1, z_2) = \frac{\lambda}{4}(z_1^2 + z_2^2)^2$.
- Example: $\lambda = e^{\frac{5i\pi}{6}}$, $K = e^{-\frac{i\pi m}{24}}$.

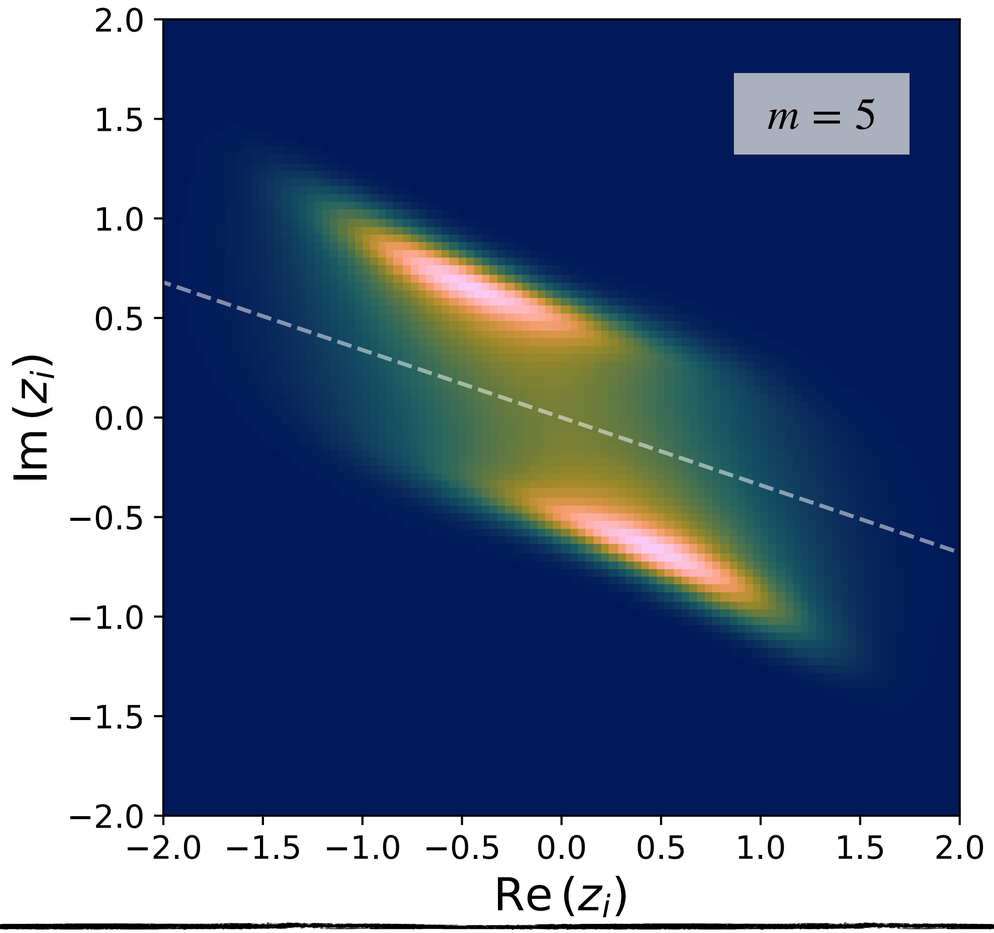

Higher dimensions

$$z_i \to z_i - \varepsilon K \frac{\partial S(z_1, z_2)}{\partial z_i} + \sqrt{\varepsilon K}\,\eta_i$$

- Consider $S(z_1, z_2) = \frac{\lambda}{4}(z_1^2 + z_2^2)^2$.
- Example: $\lambda = e^{\frac{5i\pi}{6}}$, $K = e^{-\frac{i\pi m}{24}}$.

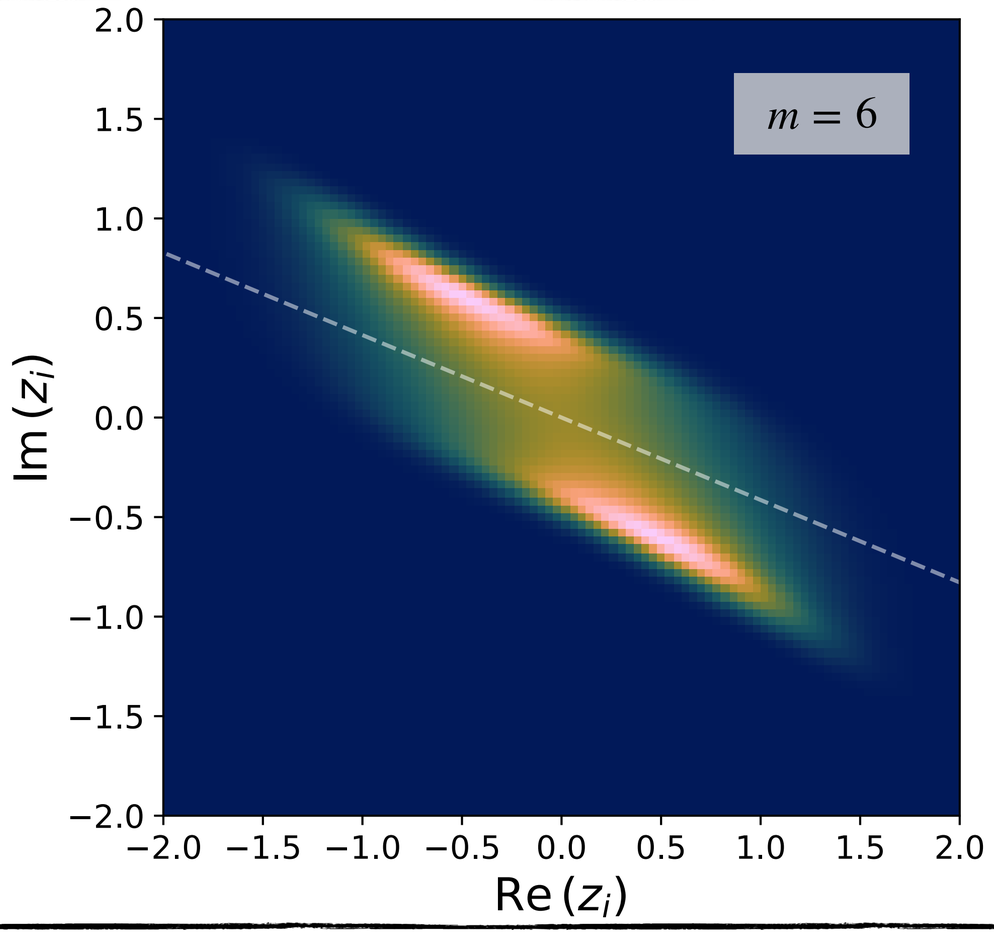

Higher dimensions

$$z_i \to z_i - \varepsilon K \frac{\partial S(z_1, z_2)}{\partial z_i} + \sqrt{\varepsilon K}\,\eta_i$$

- Consider $S(z_1, z_2) = \frac{\lambda}{4}(z_1^2 + z_2^2)^2$.
- Example: $\lambda = e^{\frac{5i\pi}{6}}$, $K = e^{-\frac{i\pi m}{24}}$.

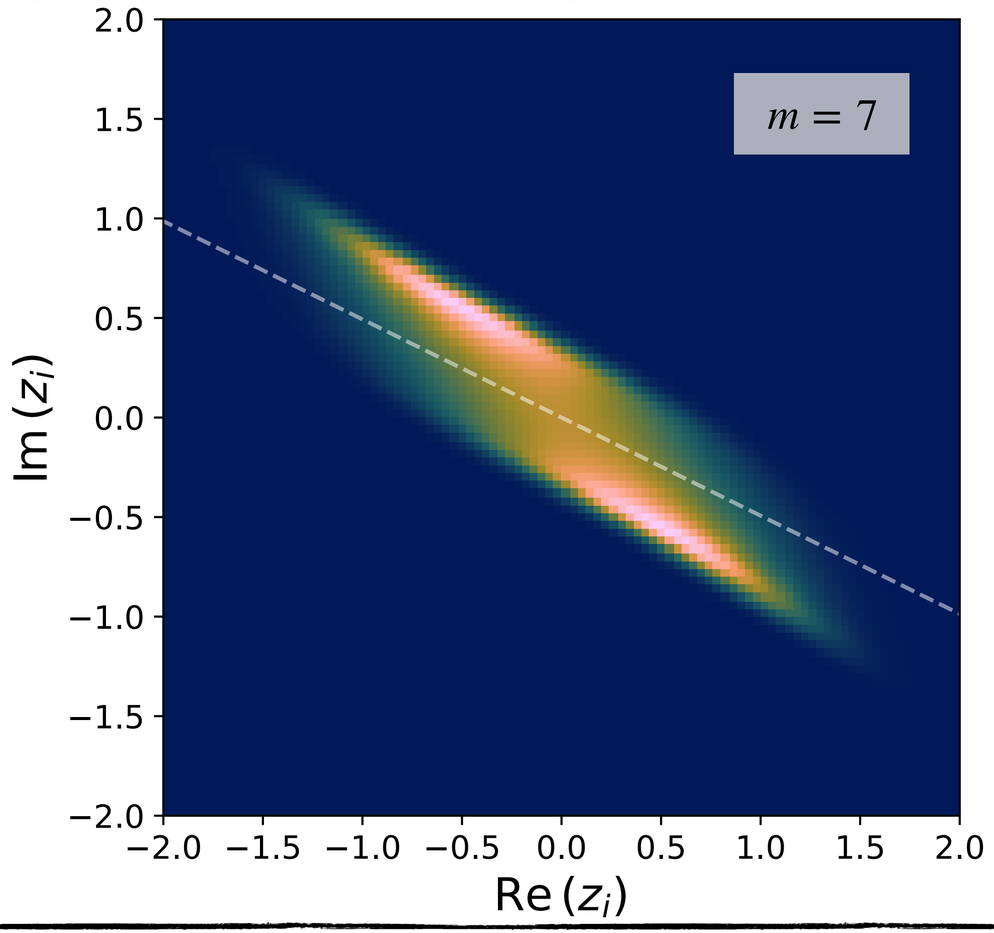

Higher dimensions

$$z_i \to z_i - \varepsilon K \frac{\partial S(z_1, z_2)}{\partial z_i} + \sqrt{\varepsilon K}\,\eta_i$$

- Consider $S(z_1, z_2) = \frac{\lambda}{4}(z_1^2 + z_2^2)^2$.
- Example: $\lambda = e^{\frac{5i\pi}{6}}$, $K = e^{-\frac{i\pi m}{24}}$.

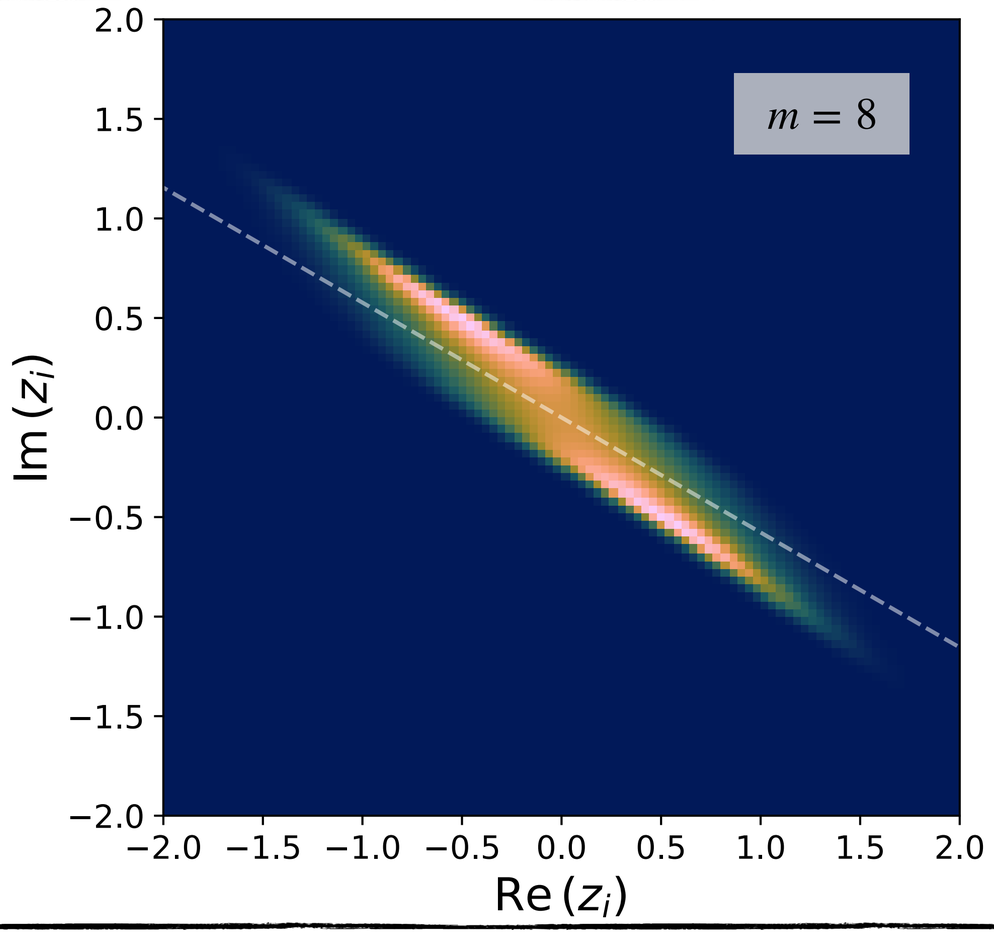

Higher dimensions

$$z_i \to z_i - \varepsilon K \frac{\partial S(z_1, z_2)}{\partial z_i} + \sqrt{\varepsilon K}\,\eta_i$$

- Consider $S(z_1, z_2) = \frac{\lambda}{4}(z_1^2 + z_2^2)^2$.
- Example: $\lambda = e^{\frac{5i\pi}{6}}$, $K = e^{-\frac{i\pi m}{24}}$.

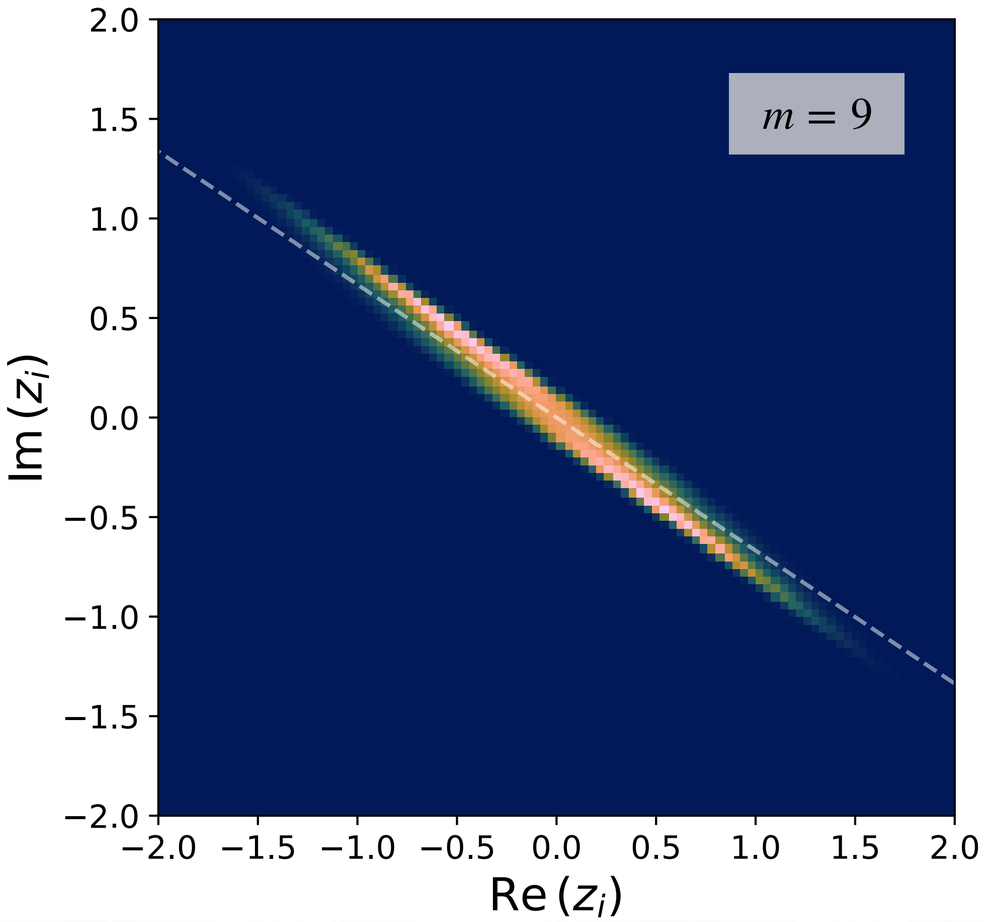

Higher dimensions

$$z_i \to z_i - \varepsilon K \frac{\partial S(z_1, z_2)}{\partial z_i} + \sqrt{\varepsilon K}\,\eta_i$$

- Consider $S(z_1, z_2) = \frac{\lambda}{4}(z_1^2 + z_2^2)^2$.
- Example: $\lambda = e^{\frac{5i\pi}{6}}$, $K = e^{-\frac{i\pi m}{24}}$.

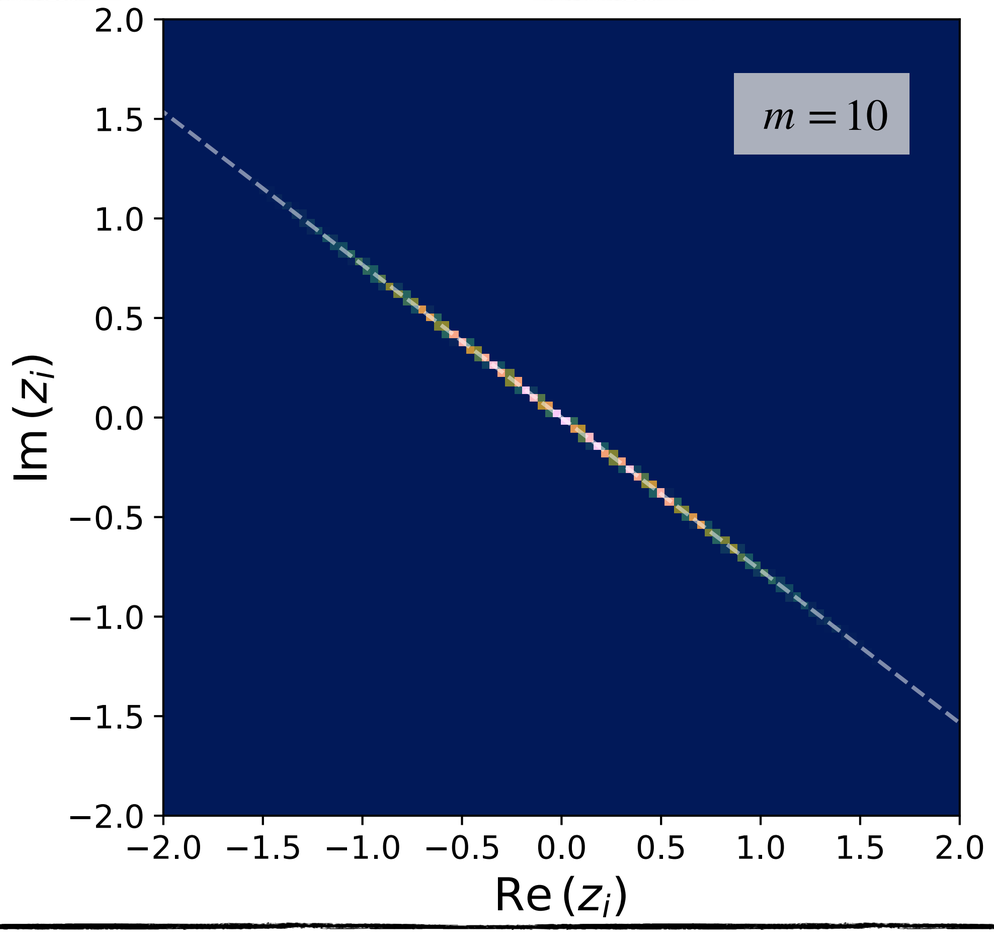

Higher dimensions

$$z_i \to z_i - \varepsilon K \frac{\partial S(z_1, z_2)}{\partial z_i} + \sqrt{\varepsilon K}\,\eta_i$$

- Consider $S(z_1, z_2) = \dfrac{\lambda}{4}(z_1^2 + z_2^2)^2$.
- Example: $\lambda = e^{\frac{5i\pi}{6}}$, $K = e^{-\frac{i\pi m}{24}}$.

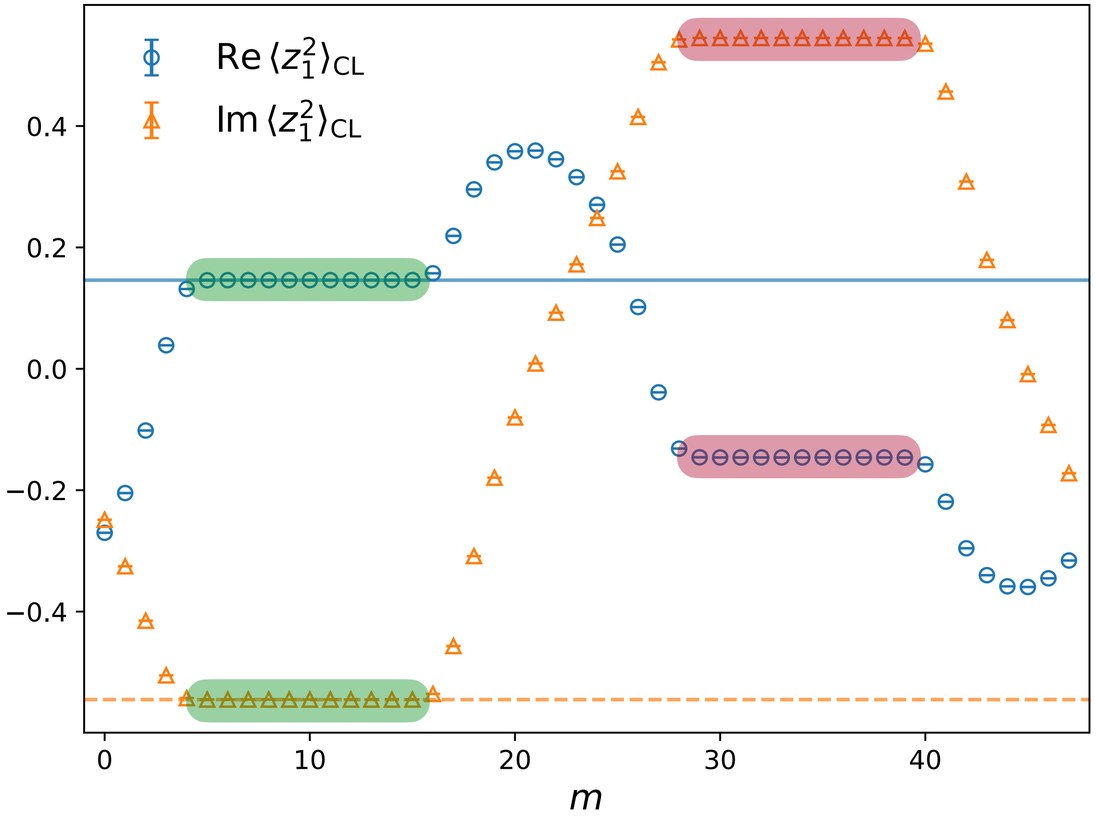

Integration cycles in higher dimensions

- $S(z_1, z_2) = \frac{\lambda}{4}(z_1^2 + z_2^2)^2$.
- $e^{-S(z_1,z_2)}$ has 8 zeros but there are only 2 independent integration cycles.
- Check validity of

$$\langle \mathcal{O} \rangle_{\mathrm{CL}} \stackrel{?}{=} a_1 \langle \mathcal{O} \rangle_{\gamma_1} + a_2 \langle \mathcal{O} \rangle_{\gamma_2}$$

- Example: $\lambda = e^{\frac{5i\pi}{6}}, K = e^{-\frac{i\pi m}{24}}$.

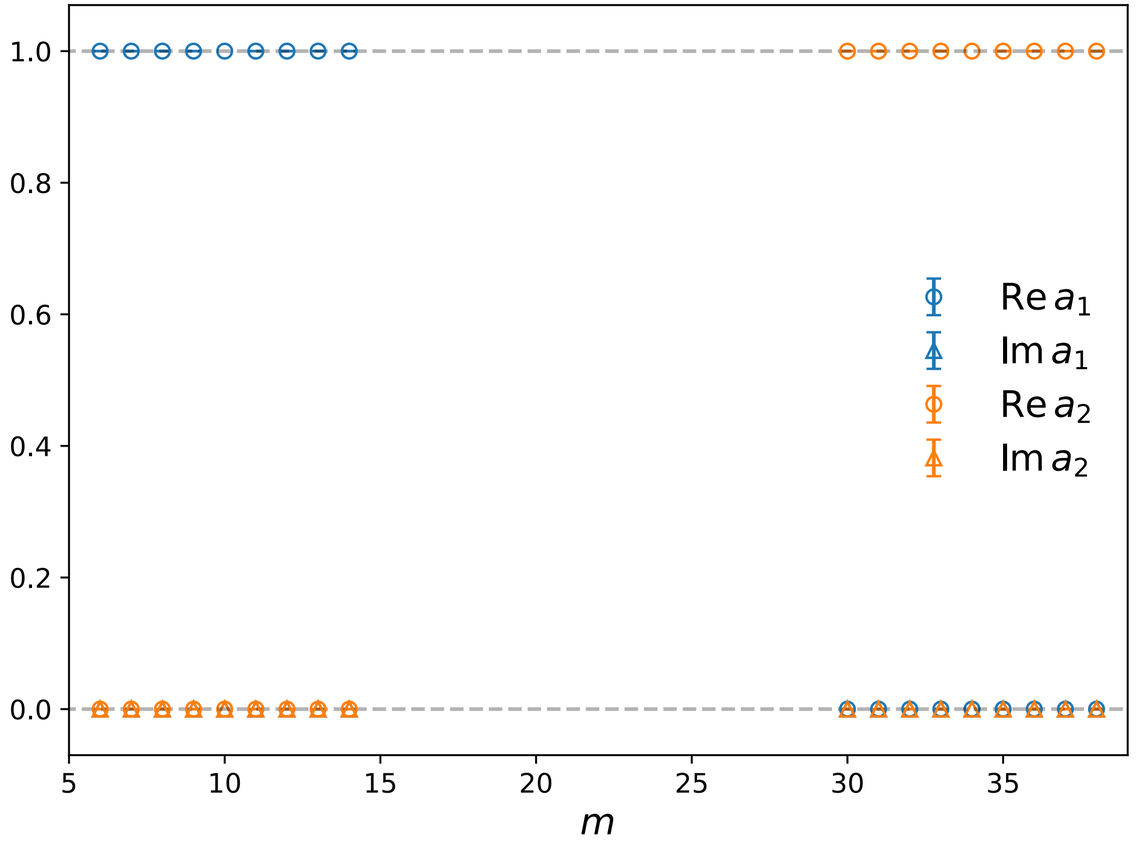

Integration cycles in higher dimensions*

- While the generalization of the concept of integration cycles to higher dimensions is not straightforward mathematically, one can still compute the number of independent cycles for a certain class of theories. In the particular model we consider on the previous slides, there are two independent cycles. This is a non-trivial finding, as it implies that the two-dimensional theory is, in fact, somewhat simpler than its one-dimensional counterpart.
- As before, we can fit the coefficients a_i and we obtain perfect agreement with the Salcedo-Seiler theorem.

Breaking O(2) symmetry

- Consider more general interactions:

$$S(z_1, z_2) = \frac{\lambda}{4}(z_1^4 + z_2^4 + a\, z_1^2 z_2^2)\,.$$

- Number of independent integration cycles depends on a.

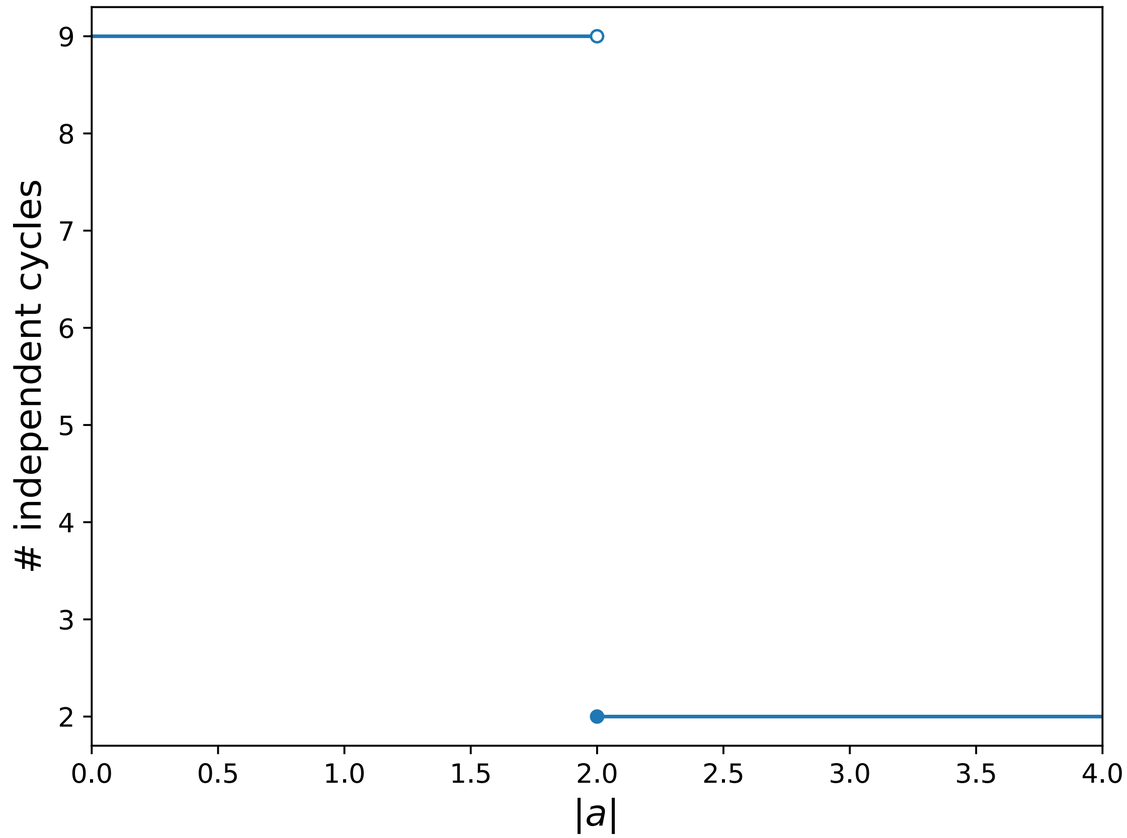

Breaking O(2) symmetry*

- If we introduce a tunable coupling parameter a into the action, the number of independent integration cycles depends on a in a crucial way: One observes a 'weak-coupling' region where there are nine independent cycles, as well as a 'strong-coupling' region in which there are only two. This could imply that more sophisticated theories in higher dimensions might actually be simpler in terms of their relevant integration cycles.

More general kernels

$$z_i \to z_i - \varepsilon K_i \frac{\partial S(z_1, z_2)}{\partial z_i} + \sqrt{\varepsilon K_i}\,\eta_i$$

- $S(z_1, z_2) = \frac{\lambda}{4}(z_1^4 + z_2^4 + a\, z_1^2 z_2^2)$.
- Example: $a = 1, \lambda = e^{\frac{5i\pi}{6}}, K_i = e^{-\frac{i\pi m_i}{24}}$.

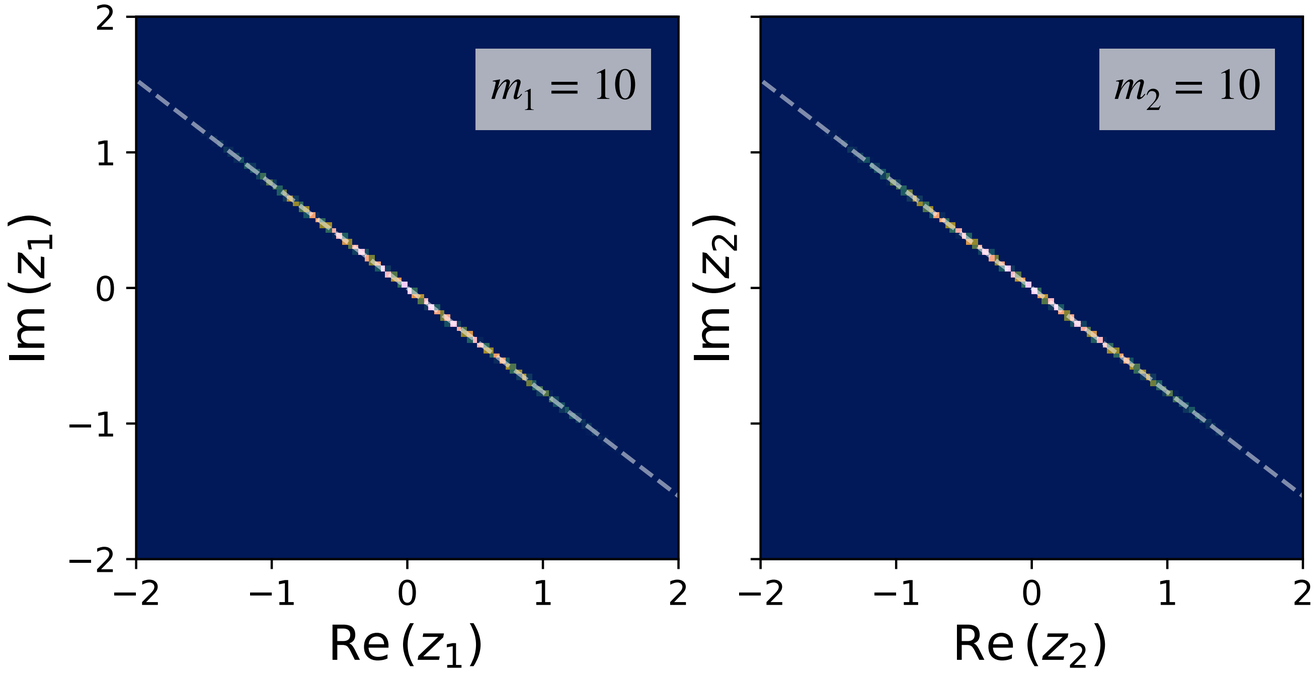

More general kernels

$$z_i \to z_i - \varepsilon K_i \frac{\partial S(z_1, z_2)}{\partial z_i} + \sqrt{\varepsilon K_i}\,\eta_i$$

- $S(z_1, z_2) = \frac{\lambda}{4}(z_1^4 + z_2^4 + a\, z_1^2 z_2^2)$.
- Example: $a = 1, \lambda = e^{\frac{5i\pi}{6}}, K_i = e^{-\frac{i\pi m_i}{24}}$.

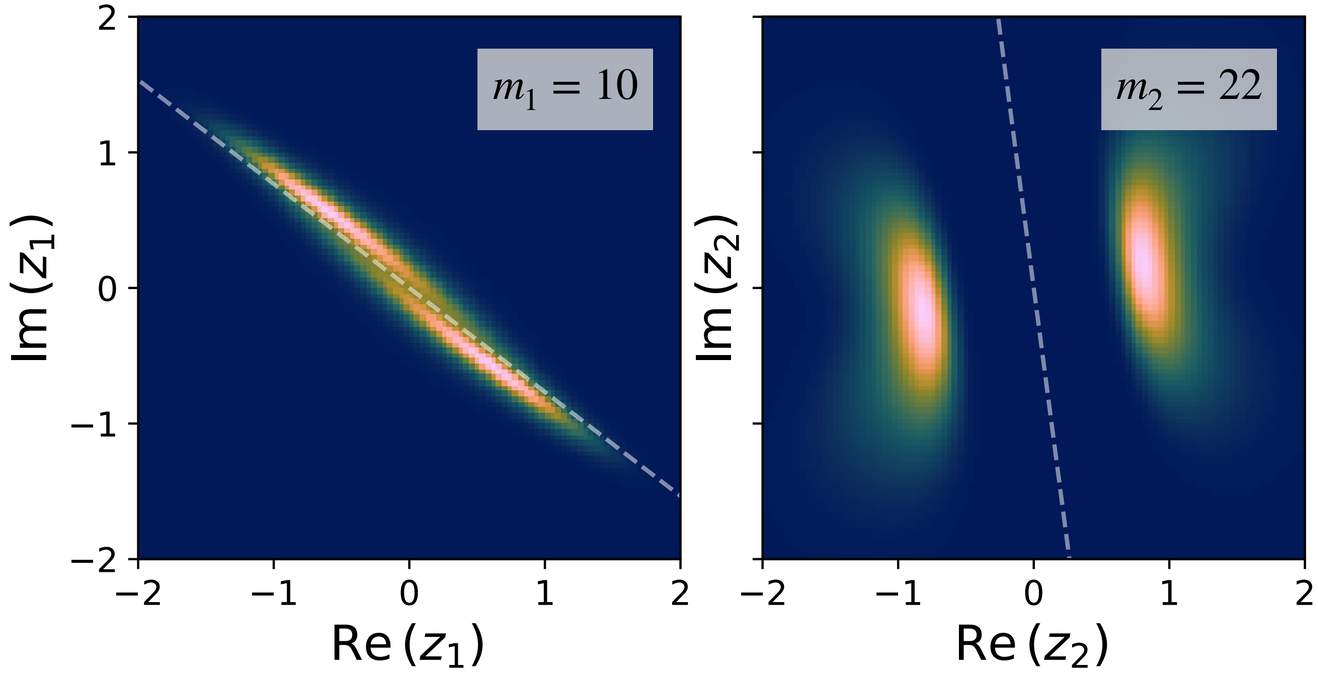

More general kernels

$$z_i \to z_i - \varepsilon K_i \frac{\partial S(z_1, z_2)}{\partial z_i} + \sqrt{\varepsilon K_i}\,\eta_i$$

- $S(z_1, z_2) = \frac{\lambda}{4}(z_1^4 + z_2^4 + a\, z_1^2 z_2^2)$.
- Example: $a = 1, \lambda = e^{\frac{5i\pi}{6}}, K_i = e^{-\frac{i\pi m_i}{24}}$.

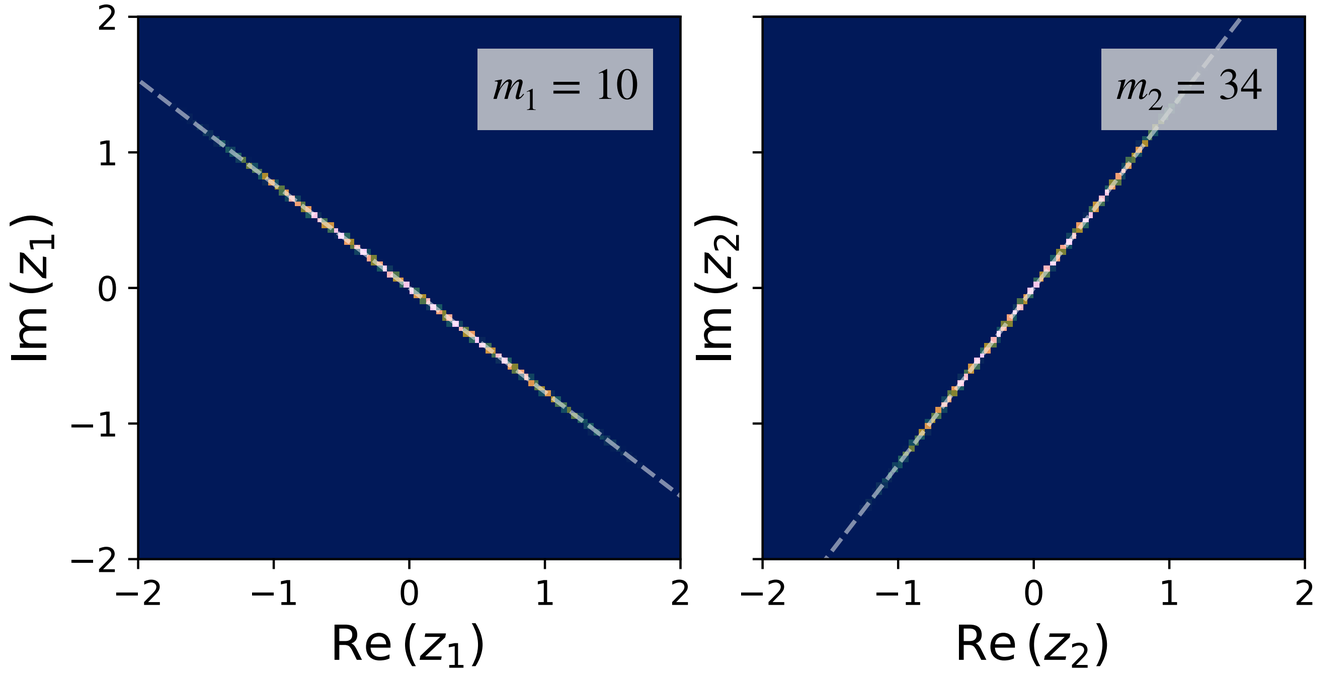

More general kernels*

- We aim at investigating which/how many of the nine independent cycles in the weak-coupling region could contribute to a simulation. To this end, we introduce more general kernels (still diagonal but now with different elements). Their effect on the distributions of z_1 and z_2 (which now no longer need to be equal) is shown on the previous slide.
- Finally, we compute the corresponding coefficients a_i. The plot on the next slide shows the contribution of the different cycles as a function of the pair of kernel parameters (m_1, m_2) and for each such pair we show two columns, the left (right) one corresponding to the real (imaginary) parts of the a_i. Different colors correspond to different coefficients and positive (negative) contributions are shown in the positive (negative) vertical directions. We find that for the sets of kernels considered, only the first four cycles are relevant.

Sampling different integration cycles

$$z_i \to z_i - \varepsilon K_i \frac{\partial S(z_1, z_2)}{\partial z_i} + \sqrt{\varepsilon K_i}\,\eta_i$$

- $S(z_1, z_2) = \frac{\lambda}{4}(z_1^4 + z_2^4 + a\, z_1^2 z_2^2)$.
- Example: $a = 0.5, \lambda = e^{\frac{5i\pi}{6}}, K_i = e^{-\frac{i\pi m_i}{24}}$.

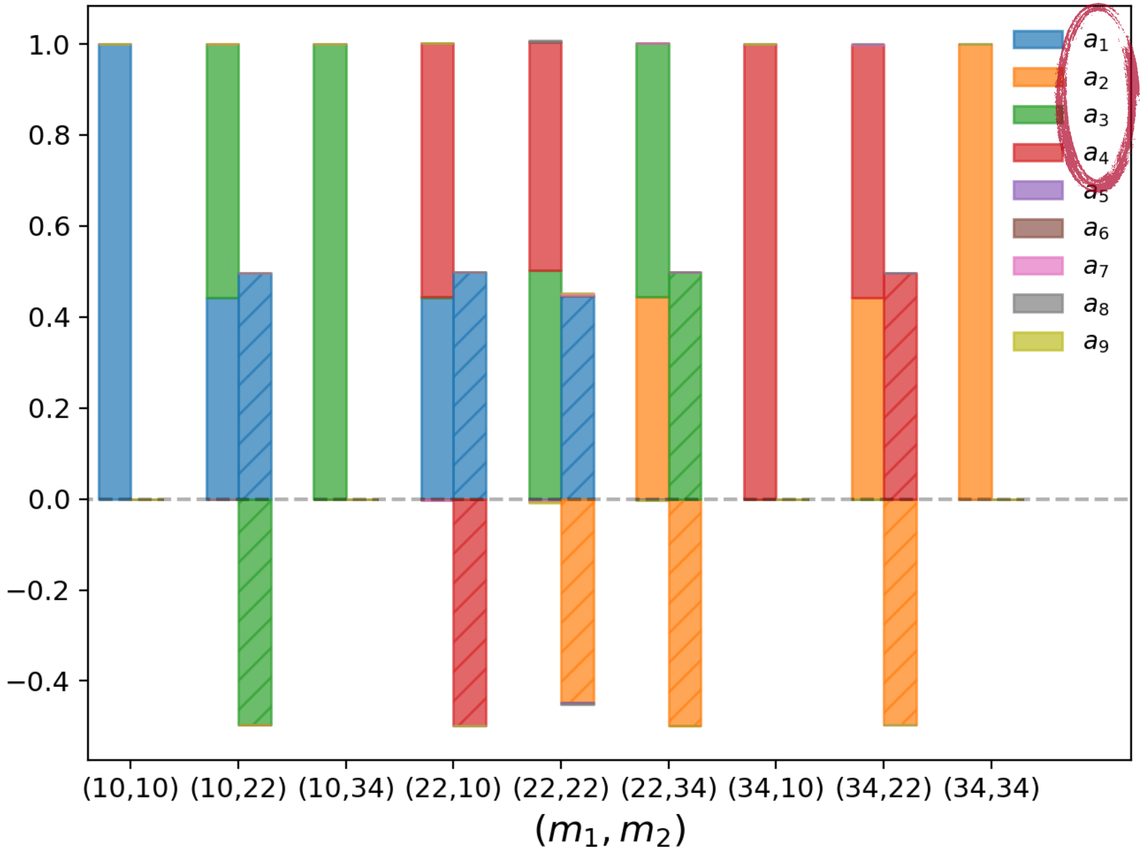

Conclusions & open questions

arXiv:2412.17137

- Evidence for validity of Salcedo-Seiler theorem beyond 1D.
- Kernel can favor certain integration cycles.

- Complex Langevin can be extended to theories of physical interest.
- Also there, kernels are possible. But how to choose them?
- What about integration cycles in realistic theories?

Summary & Outlook

- CL promising approach for systems with a complex-action problem.
- Major drawbacks: Runaways (adaptive step size) and wrong convergence.
- Wrong convergence can in principle be fixed by kernels.
  - How to construct them?
  - How to verify convergence?
- Outlook: Role of integration cycles in realistic theories?

Contact*

- For any questions/discussion, please do not hesitate to contact the author via michael.mandl@uni-graz.at .